1-31-1992

Series compensation investigation on the hydro-quebec and NYPA 765 kV transmission system : modeling and stability analysis

Hans J. Candia
New Jersey Institute of Technology

ABSTRACT

Title of Thesis:	*Series Compensation Investigation on the Hydro-Quebec and NYPA 765 kV Transmission System: Modeling and Stability Analysis*
Name and Degree:	*Hans J. Candia* *Master of Science* *in Electrical Engineering, 1992* *New Jersey Institute of Technology*
Thesis Directed by:	*Dr. S. B. Pandey* *Asst. Professor of E.E.*

This thesis presents a mathemathical approach for raising the power steady state stability limit by adding series capacitive compensation to a transmission line. The effect of series capacitive compensation and degree of compensation were investigated in detail. The power system studied includes an automatically controlled power system, IEEE Type I.

The results of the actual and theoretical steady state stability limits for a given series capacitance location and degree of compensation were obtained by applying the frequency domain technique. The natural frequencies of each compensated power network were examined.

The best location for series capacitive compensation is proposed which is the midpoint of the MSU-1 and MSC-7040 lines. At this location, the actual and theoretical power steady state stability limits were obtainedand compared for different degrees of compensation and system operating voltages.

Approved by: ______________________

Dr. S. B. Pandey

SERIES COMPENSATION INVESTIGATION

ON THE

HYDRO-QUEBEC and NYPA 765 kV

TRANSMISSION SYSTEM:

MODELING AND STABILITY ANALYSIS

by
Hans J. Candia

Thesis submitted to the Faculty of the Graduate School
of the New Jersey Institute of Technology for the degree of
Master of Science in Electrical Engineering

1992

APPROVAL SHEET

Title of Thesis: Series Compensation Investigation on the Hydro-Quebec and NYPA 765 kV Transmission System: Modeling and Stability Analysis

Name of Candidate: Hans J. Candia
Master of Science in
Electrical Engineering, 1992

Thesis and Abstract Approved:

1/8/92

Dr. S. B. Pandey — Date
Asst. Professor of E.E.
N. J. I. T.

Other members of the thesis review committee:

1/8/92

Dr. Edwin Cohen
Professor of E. E.
N. J. I. T.

1/8/92

Dr. Yun-Quing Shi
Asst. Professor E. E.
N. J. I. T.

1/8/92

Dr. Betzalel Shperling
Senior Electrical Engineer
New York Power Authority

VITA

Name: HANS J. CANDIA

Premanent address: 268 Griffith Street
Jersey City, N. J. 07307

Degree and date to be conferred: MSEE, May 1992

Date of birth:

Place of birth:

Secondary Education: "Colegio Santa Rosa de Lima",
High School Diploma, Dec., 1974

Collegiate institutions attended:	Dates	Degree/dates:
New Jersey Institute of Technology	1988-1992	MSEE/1992
New Jersey Institute of Technology	1977-1981	BSEE/1981
Essex County College	1975-1977	

Major: Electrical Engineering

Position held: Senior Electrical Engineer
New York Power Authority
123 Main St.
White Plains, N. Y. 10601

Acknowledgment

I would like to express my sincere gratitude to Dr. S. B. Pandey for his teaching, support and guidance during the completion of this thesis.

I would also like to thank my wife for her encouragement and support during the time of my thesis work.

Table of Contents

Appendix I.

Beauharnois Generators Data

Appendix II

Beauharnois Step-Up Transformers Data

Appendix III

MSU-1 and MSC-7040 Line Data

Appendix IV

Parameters of System Studied in Common MVA Base

List of Figures

List of Tables

List of Symbols

E	Effective emf
E'	Transient emf
E_q	Quadrature-axis component of E
E'_q	Quadrature-axis component of E'
f	Operating frequency
I_{act}	Active current component
I_d	Direct-axis component
I_q	Quadrature-axis current
I_{react}	Reactive current component of current
P	Active power
p	Time derivative operator
Q	Reactive power
V	Voltage
V_d	Direct-axis voltage
V_q	Quadrature-axis voltage
x_d	Direct-axis synchronous reactance
x'_d	Transient reactance
x_q	quadrature reactance
x_e	transfer reactance
$x_{d\Sigma}$, $x'_{d\Sigma}$, $x_{q\Sigma}$	total reactances
δ	load angle
ψ	angle between voltace and current

ψ	*Angle between emf and current*
T_{do}	*Time constant field winding open-circuit*
T'_d	*Direc-axis transient time constant*
T_3	*Time constant of rectifier*
T_e	*Time constant of exciter*
K_e	*Exciter gain*
P_1, P_2, P_3	*Power derivatives*
S_1, S_2, S_3	*Power derivatives*
K_{ov}	*AVR gain control for a proportional channel*
M	*Inertia constant*
P_e	*Electric output from the generator*
E_q	*Internal voltage behind the reactance*
E'_q	*Internal voltage behind the reactance*
E_{qe}	*Correction voltage by AVR action*
V_s	*Voltage operating signal*
$\Delta\delta$	*Angle operating signal*

CHAPTER I

1.1 Introduction

Continued demand growth from the load areas which are remote from generating stations, combined with limited generation or transmission line right-away expansion are some problems of power system planning. These problems are some of the considerations which merit the planning of power transmission system compensation to increase the power transfer between generation and load areas.

A recommendation was made at the Symposium of Subsynchronous Resonance (SSR) held at the IEEE PES Summer meeting of 1975, that system planners give more consideration to shunt compensation for improvements of stability limits [3]. The main reason behind this recommendation was that shunt capacitors give rise to super-synchronous natural frequencies and therefore do not produce a risk of SSR, but they produce objectionable overvoltages at light loads.

But E. W. Kimbark has suggested that series capacitor appear preferable where generation is hydro or where enough load is present to ensure adequate damping of subsynchronous natural frequencies [3]. It is true that the natural frequencies of circuits with series capacitors are subsynchronous and therefore the use of series capacitors involves certain risk of subsynchronous resonance which has been known to produce serious mechanical damage to turbogenerator sets.

1.2 Objectives

The objective of this thesis is to describe with a mathematical approach the increase of the power steady state stability limits (P_{SSSL}) of an automatically controlled power system using series capacitive compensation with respect to the location on the line and the degree of compensation. The natural subsynchronous frequency of each network investigated are also presented. The power system studied includes the Hydro-Quebec's Beauharnois generating complex connected to the New York Power Authority (NYPA) 765 kV transmission system whose details are presented in the next section. The power stability limits can be obtained by applaying the frequency domain technique in terms of the automatic excitation regulator (AER) adjustable parameter. The actual steady state stability limits are obtained by testing the system's stability locus with the Routh-Hurwitz criteria. The maximum theoretical power transfer limit is also presented.

1.3 *Description of the System Studied*

The existing 765Kv interconnection between Hydro-Quebec (HQ) and New York Power Authority (NYPA) consists of the Chataguey-Beauharnois generation complex and the Marcy substation, which is located 194 miles south in New York.

The HQ Chataguey-Beauharnois hydro-generation station is mainly radially operated to export energy from Canada to New York state. The generators at this station utilize IEEE type I excitation control system. Power is first carried by HQ's MSC-7040 365Kv line to NYPA's Massena substation, 55.8 miles from the Chataguey substation. From the Massena site, the power is further carried 138 miles to NYPA's Marcy 765Kv substation via the MSU-1 line. The Chataguey 765Kv substation is interconnected with the HQ main 735Kv system and the Massena substation with NYPA's 230Kv network via two autotransformers. These interconnections to the HQ-NYPA 765Kv systems are mainly used to support Beauharnois generation when necessary. Figure 1 shows the overall interconnection of the 765Kv system.

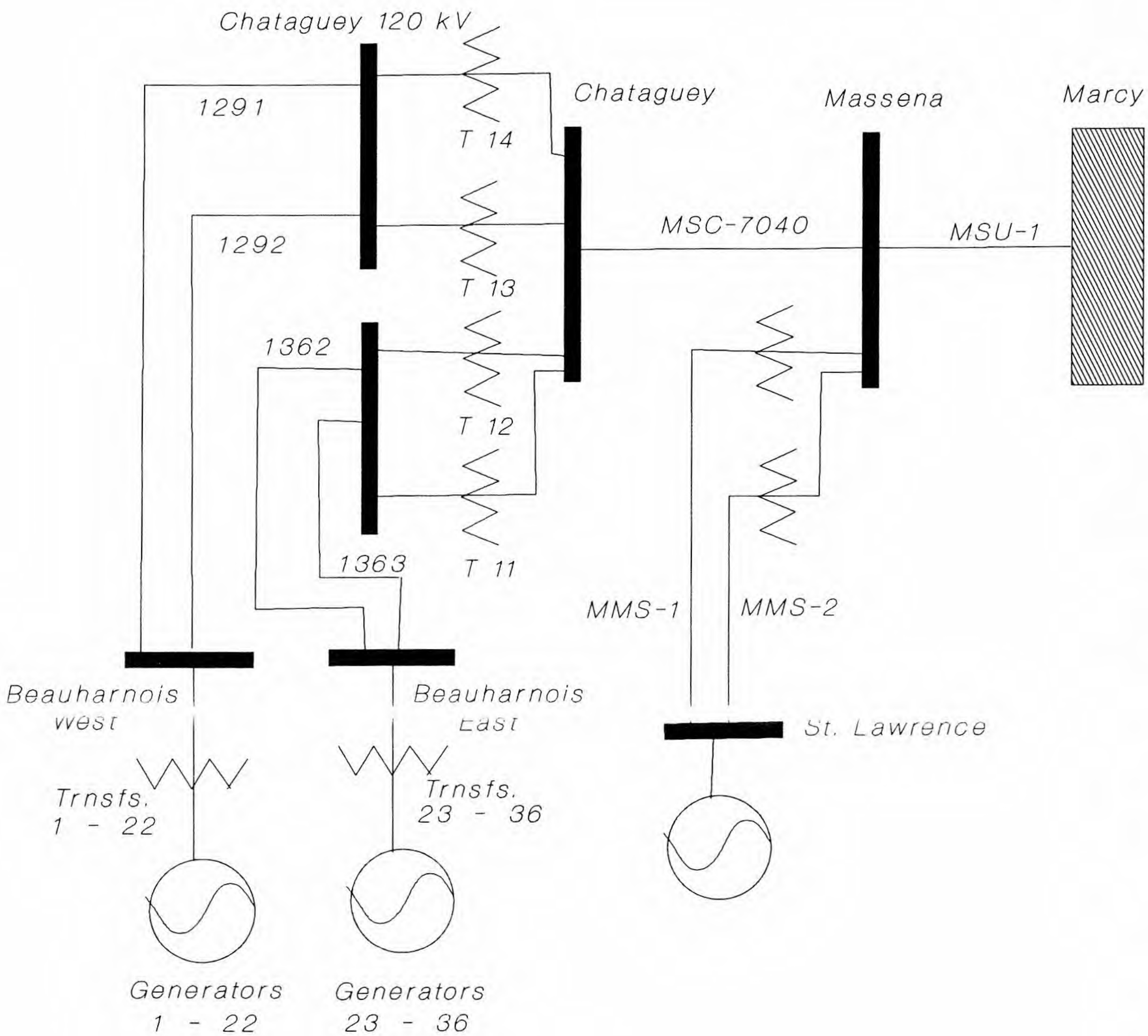

Chataguey 120 kV
1291
T 14
Chataguey
Massena
Marcy
1292
MSC-7040
MSU-1
T 13
1362
T 12
1363
T 11
MMS-1
MMS-2
Beauharnois
West
Beauharnois
East
St. Lawrence
Trnsfs.
1 - 22
Trnsfs.
23 - 36
Generators
1 - 22
Generators
23 - 36

Figure 1

1.4 Plan of Thesis

Chapter I introduces the problem investigated, describes the system studied and outlines the objectives of this thesis.

Chapter II presents an overview of series capacitance compensation and the excitation system of the hydro-generating station studied.

Chapter III describes the assumptions made, mathematical linearized models, algorithms developed, and the computer simulation program strategy used to evaluate the system's stability. Frequency domain technique is proposed and used in the analysis.

Chapter IV presents the details of the system studied, calculation details of various variables needed in the analysis for the uncompensated and compensated cases.

Chapter V presents a discussion of the results and analysis

Chapter VI conclusions

CHAPTER II

Overview of the Series Capacitance Compensation and Automatic Excitation Regulator Control System

2.1 Series Capacitance Compensation.-

The improvement of a power stability limit on a system can be obtained by reducing the overall transfer impedance between the sending and receiving ends of a power system. The following methods are available to decrease a system's transfer impedance:

- Reducing the reactance of generators by increasing the number of generators
- Reducing the reactance of step-up transformers by increasing the number of parallel transformers
- Reducing transmission line impedence by increasing the number of parallel lines
- Adding series capacitance compensation

Series capacitance compensation offers the most economical solution when compared to the other alternatives. Series capacitance compensation approach is applied and investigated to the 765Kv interconnection between HQ and NYPA.

From the circuit shown below on figure 2, we can demonstrate how series compensation will reduce the transfer impedence and increase the line power transfer capability.

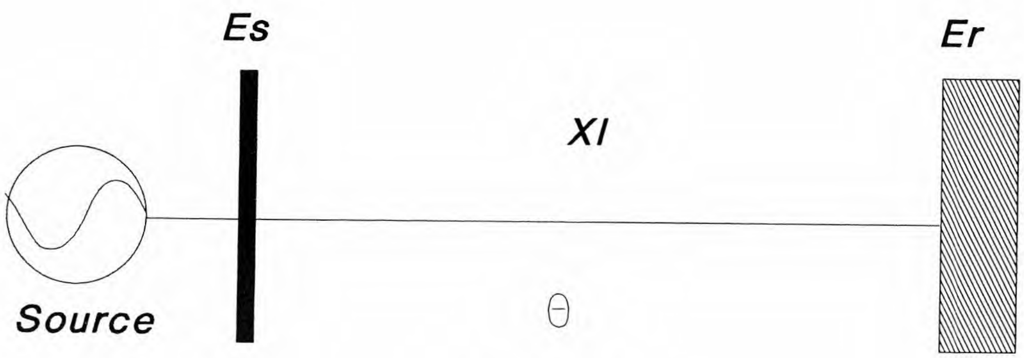

Figure 2

ignoring system losses:

$$P = \frac{E_s \, E_r \, \sin\theta}{X_l} \qquad (2.1)$$

where:

E_s *is the sending end voltage*

E_r *is the receiving end voltage*

X_l *is the transmission line impedance*

0 *is the angle between the sending and receiving end voltages*

For $0 = 90$

$$P_{max} = \frac{E_s \ E_r}{X_l} \tag{2.2}$$

and with $E_s = E_r = 1.0pu$ *and* $X_l = 1.0pu$*, we get*

$$P_{max} = 1.0 \text{ p.u.} \tag{2.3}$$

Now, if we reduce the effective line reactance by introducing series capacitance, then the maximum power transfer capability is given by.

$$P_{max} = \frac{E_s\ E_r}{X_l\ -\ X_c} \qquad (2.4)$$

where X_c is the capacitor impedence.

Let X_c = 50% of X_l then

$$P_{max} = \frac{E_s\ E_r}{X_l - X_c} = \frac{E_s\ E_r}{X_l - .5X_l} = \frac{E_s E_r}{.5X_l} \qquad (2.5)$$

and with $E_s = E_r = 1.0pu$ and $X_l = 1.0pu$, we will have

$$P_{max} = 2.0\ p.u. \qquad (2.6)$$

The power angle characteristics of both compensated and uncompensated lines are given in figure 3.

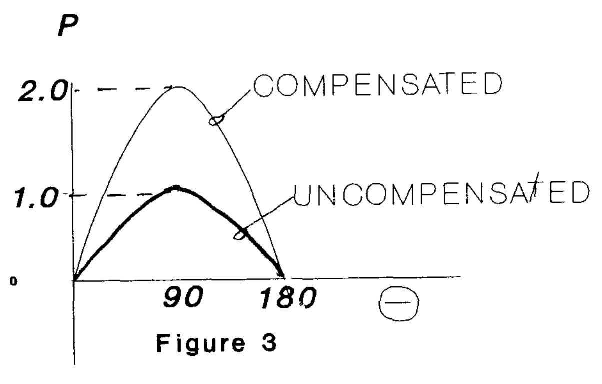

Figure 3

In addition to improving the power stability limit, series compensation has been found effective in :

- *Changing load divisions on parallel paths*
- *Enabling better controls of line load levels*
- *Reducing transmission losses*
- *Reducing voltage drops during system disturbances*

While employing series capacitors, care must be taken to limit the increase current levels, subharmonic frequencies or subsynchronous resonance levels within acceptable values.

The percent line compensation can be defined as

$$\% \text{ compensation} = \frac{X_C}{X_l} * 100 \tag{2.7}$$

The percentage of compensation varies between 20% and 80%. It has been demonstrated that a minimum of 20% compensation is required to justify economic investment. Levels higher than 80% of compensation increase the available fault current levels, the subsynchronous resonance (SSR) and subharmonic frequencies. This requires higher insulation levels in equipment, which is not economically feasible.

The natural frequency of a compensated line can be calculated from

$$f_n = f\sqrt{\frac{X_c}{X_l}} \tag{2.8}$$

Since X_c/X_l is between 20% and 80%, f_n will be of subharmonic nature of the power frequency, f. The subharmonic frequencies can give rise to transient currents which may be damped out in a few cycles or may last significantly longer. The transient currents may also excite one or more torsional frequencies on the mechanical shaft of the generator, the phenomenon is referred to as subsynchronous resonance (SSR). These torsional oscillations may be severe enough to damage the generator shaft.

2.2 Automatic Excitation Regulator Control System.-

Synchronous generators and its associated turbines must operate to ensure normal conditions in the system by maintaining its operation between certain limits. Excitation Regulators control the voltage output of the synchronous generator. Speed governors and frequency regulators control the frequency of the generators between its limits. To determine the stability of an automatically controlled power network, the excitation control system characteristics must be modeled appropriately, especially when stability results are sought in terms of gain controlling parameters.

An "Excitation Regulating Control System" is a combination of devices designed to generate a field current which is applied to the rotating field of the electric machine (rotor) and then induced a voltage in the stator of the machine. This field current is controlled by means of manual or automatic control. To explain the process of excitation control, let us refer to figure 4.

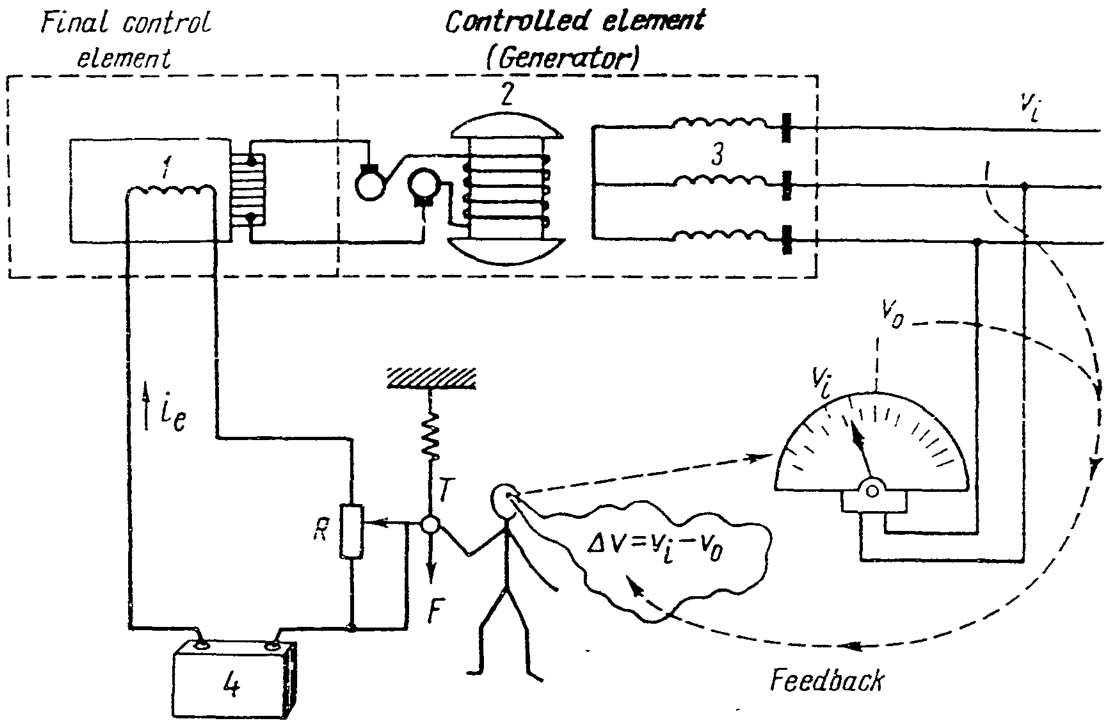

Figure 4

From figure 4, we can see that the signal V_i is constantly fed to a voltmeter with a reference voltage V_o. The difference of V_i and V_o is a ΔV voltage which is the error signal to be corrected. The control to the field I_e is obtained by adjusting the rheostat R by manual or automatic means.

The manual control system is also known as "control with a dead zone". The manual adjustment will be done by an operator which obviously cannot respond to a small change. Therefore, a range of V must be established, i.e., $V < \Delta V'o < Vo$ which is the dead zone. The operator will have to respond to a $V'o$ value and adjust the rheostat accordingly.

An automatic control will respond to an infinitely small change and will adjust the rheostat accordingly. This automatic control is also called "proportional control". There are also several types of excitation systems which are classified by industry standards,such as the IEEE [1] classification:

IEEE Type 1: Continuously Acting Regulator and Exciter

This type of excitation is of the proportional type where the Adjustable Excitation Rectifier (AER) control will respond continuously to changes in the output voltage.

We would like to point out here that the H-Q hydrogenerators at the Beauharnois station employ this type of excitation control systems.

IEEE Type 2: Rotating Rectifier System

This type of AER uses a damping loop input from the regulator output.

IEEE Type 3: Static with Terminal Potential and Current Supplies

This type of AER also uses a current input to control its excitation level. A current reference is also required with this type of AER.

IEEE Type 4: Noncontinuous Acting

This is a fast acting, high gain AER. This system has two different control systems. Depending on the V magnitude error the different controls are applied. For small errors adjustments are made with a motor-operated rheostat. For large errors the adjustments are made by applying Vrefmax or Vrefmin to the exciter.

The functional block diagram for the four types of AER's are shown on figures 5 through 8 respectively.

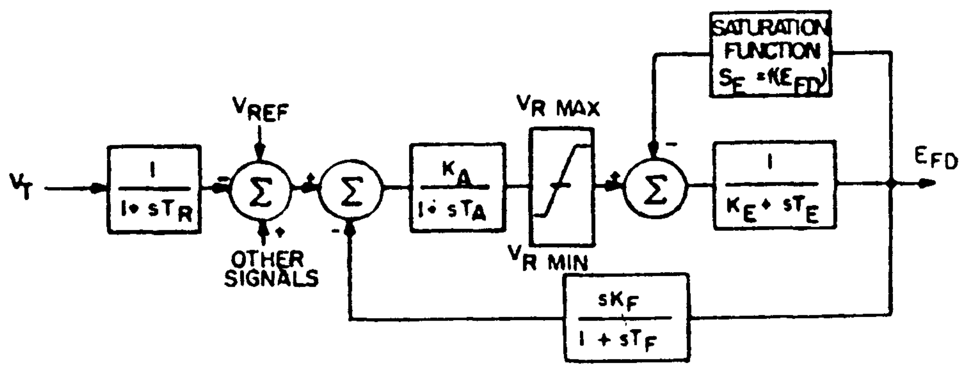

Fig. 5 . Type 1 excitation system representation, continuously acting regulator and exciter.

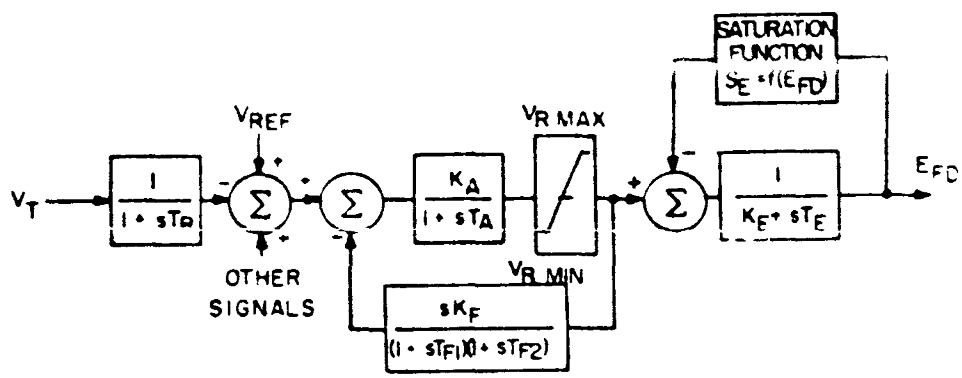

1

Fig. 6. Type 2 excitation system representation, rotating rectifier system.

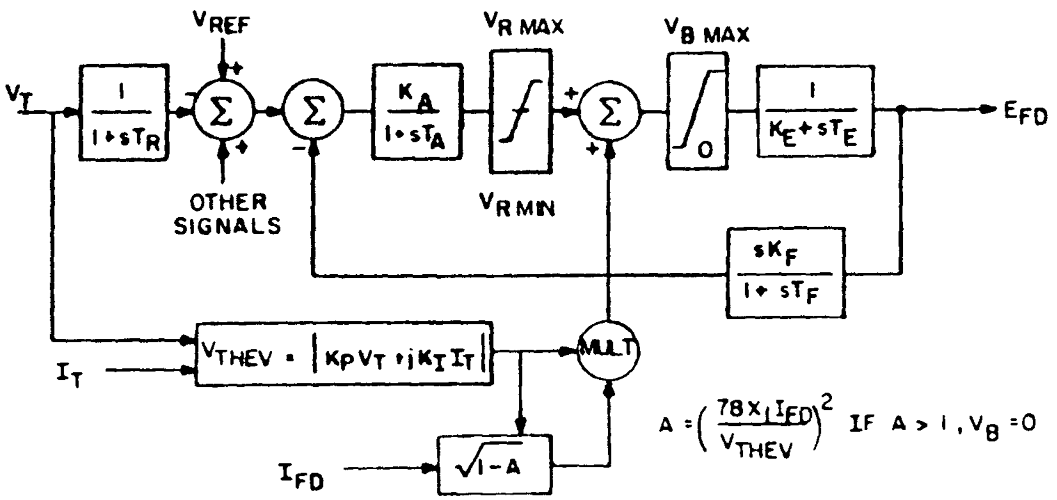

Fig. 7 Type 3 excitation system representation, static with terminal potential and current supplies.

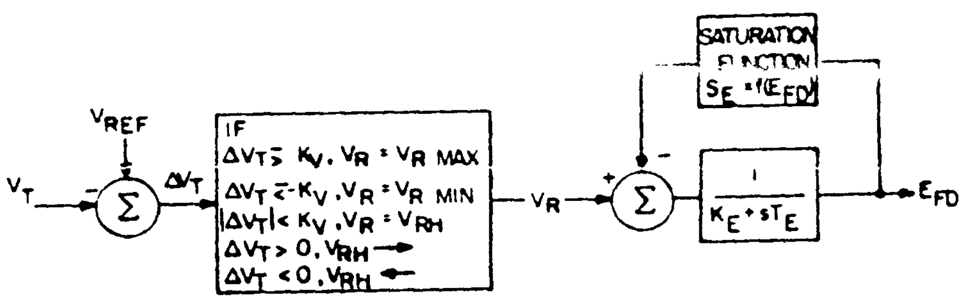

Fig. 8 Type 4 excitation system representation, noncontinuously acting regulator. *Note:* V_{RH} limited between $V_{R\,min}$ and $V_{R\,max}$. Time constant of rheostat travel T_{RH}.

CHAPTER III

Analysis

3.1 Assumptions Made

The following assumptions were made in the analysis:

(a) Effect of governor-action and generator winding damping were ignored.

(b) Saturation of exciter and main generator were not included.

(c) Effect of feedback compensating network of IEEE excitation control system type I is not included.

(d) Since the total generated power is much less, compared to the demand, the H Q NYPA 765Kv is modelled as one machine system.

(e) MMS-1 and MMS-2 lines were not accounted for in this study.

(f) All circuit parameters are lumped and assumed to remain constant during the small period of oscillations

3.2 Linearized Models

This section describes the linearized models for the H-Q generator excitation system and power network elements.

3.2.1 Hydrogenerator

An equivalent hydrogenerator can be modeled by the dynamic model simulating the slow changes of its electromagnetic and electromechanical changes. The model representing slow changes in the excitation winding can be derived using d-q transformation as:

$$\Delta E_{qe} = \Delta E_q + T_{do}\, p\, \Delta E'_q \qquad (3.1)$$

where E_{qe} represents the change in voltage applied to the generator excitation winding.

The dynamic model for a generator, which includes the electro-mechanical equation for the rotor is given as[20]:

$$M \frac{d^2 \Delta \delta}{dt^2} + \Delta P_e = 0 \qquad (3.2)$$

3.2.2 Automatic Excitation Control System (IEEE Type I)

The main excitaiton of the H-Q generatprs is controlled by a voltage actuated automatic exitation regulator (AER) which has one proportional gain control channel. The output of the exciter field system provides the neccesssary correction to the generator main field winding.Based on the assumtions for the AER, the block diagram of figure 5 can be symplified as shown in figure 9, its matemathical model form is:

$$\Delta E_{qe} = \frac{-\,K_{ov}\;\; K_e \Delta V_s}{(1+pT_e)(1+pT_3)} \qquad (3.3)$$

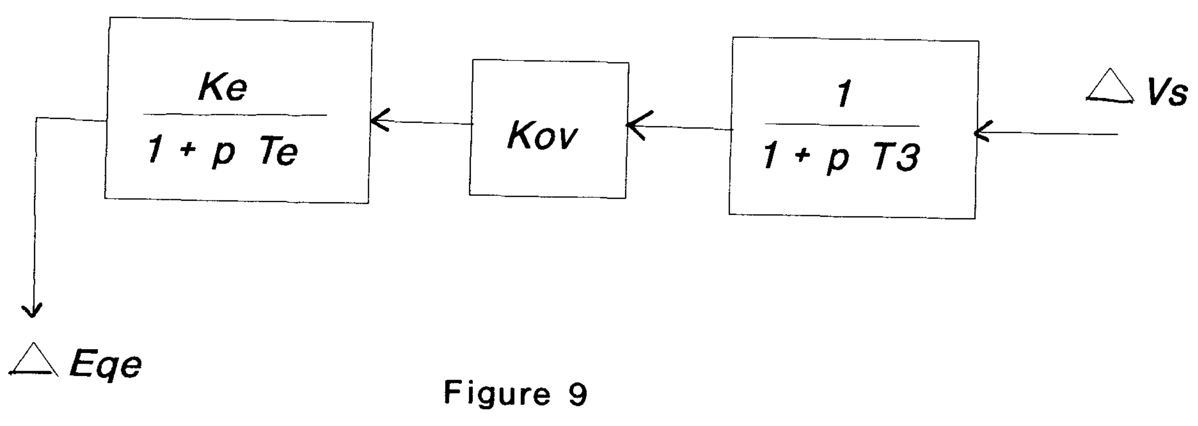

Figure 9

3.2.3 Power Output Models

The following power output expressions can be derived from the phasor diagram of figure 10, expressing them in partial derivatives form.

$$\Delta P_{Eq} = P_1 \Delta E_q + S_1 \Delta \delta \tag{3.4}$$

$$\Delta P_{E'q} = P_2 \Delta E_q' + S_2 \Delta \delta \tag{3.5}$$

$$\Delta P_{Vs} = P_3 \Delta V_s + S_3 \Delta \delta \tag{3.6}$$

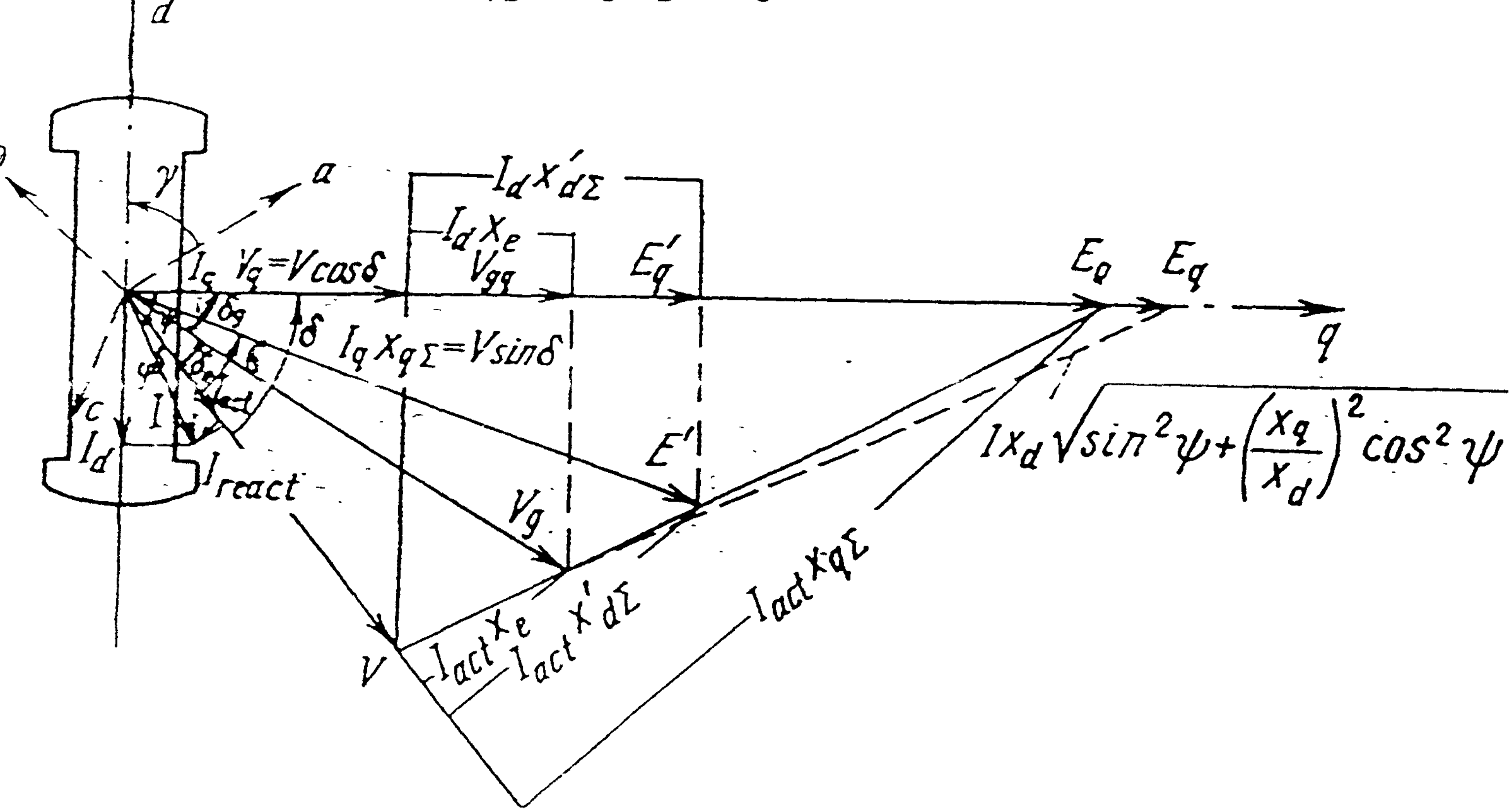

Figure 10

where,

$$P_1 = \frac{\partial P_{Eq}}{\partial E_q} \tag{3.7}$$

$$S_1 = \frac{\partial P_{Eq}}{\partial \delta} \tag{3.8}$$

$$P_2 = \frac{\partial P_{E'q}}{\partial E'_q} \tag{3.9}$$

$$S_2 = \frac{\partial P_{E'q}}{\partial \delta} \tag{3.10}$$

$$P_3 = \frac{\partial P_{Vs}}{\partial V_s} \tag{3.11}$$

$$S_3 = \frac{\partial P_{Vs}}{\partial \delta} \tag{3.12}$$

and P_{Vs}, P_{Eq} and $P_{E'q}$ are active powers at the generator bus which are equal to P_e.

3.3 Overall System Performance Equation with Type 1 Excitation Control System

Let equation 3.3 be rewritten as

$$\Delta E_{qe} = \frac{-A \,\Delta V_s}{B} \qquad (3.13)$$

where

$$A = K_{ov} \, K_e$$

$$B = 1 + p(T_3 + T_e) + p^2 T_3 T_e \qquad (3.14)$$

or,

$$B = p^2 B_0 + pB_1 + B_2 \qquad (3.15)$$

then,

$$B_0 = T_3 T_e \qquad (3.16)$$

$$B_1 = T_3 + T_e \qquad (3.17)$$

$$B_2 = 1 \qquad (3.18)$$

Substituting 3.2 into equation 3.4,

$$- Mp^2 \Delta\delta = P_1 \Delta E_q + S_1 \Delta\delta \qquad (3.19)$$

simplifying

$$\Delta E_q = \frac{-(Mp^2 + S_1)}{P_1} \Delta\delta \qquad (3.19a)$$

Substituting 3.2 into 3.5,

$$-Mp^2\Delta\delta = P_2\Delta E_q' + S_2\Delta\delta \qquad (3.20)$$

simplifying

$$\Delta E_q' = \frac{-(Mp^2 + S_2)}{P_2} \Delta\delta \qquad (3.20a)$$

Substituting 3.19a and 3.20a into 3.1,

$$\Delta E_{qe} = -\left(\left(\frac{S_1 + Mp^2}{P_1}\right) + T_{do}\, p \left(\frac{Mp + S_2}{P_2}\right)\right)\Delta\delta \qquad (3.21)$$

Factoring P_1

$$\Delta E_{qe} = \frac{-1}{P_1}\left(S_1 + Mp^2 + T_{do}p\frac{P_1}{P_2}(Mp + S_2)\right)\Delta\delta \qquad (3.22)$$

simplifying the above expression,

$$\Delta E_{qe} = \frac{-1}{P_1}\left(T_{do}p\frac{P_1}{P_2}Mp^3+Mp^2+T_{do}p\frac{P_1}{P_2}MpS_2+S_1\right)\Delta\delta \tag{3.22a}$$

The polynomial inside the brackets is then replaced as C,then

$$\Delta E_{qe} = \frac{-C}{P_1}\Delta\delta \tag{3.23}$$

where,

$$C = C_0p^3 + C_1p^2 + C_2p + C_3 \tag{3.24}$$

where,

$$C_0 = T_{do}\ M\ \frac{P_1}{P_2} \tag{3.25a}$$

$$C_1 = M \tag{3.25b}$$

$$C_2 = T_{do}\ \frac{P_1\ S_2}{P_2} \tag{3.25c}$$

$$C_3 = S_1 \tag{3.25d}$$

Substituting 3.2 into equation 3.6,

$$-M\ p^2\Delta\delta = P_3\Delta Vs\ +\ S_3\Delta\ \delta \qquad (3.26)$$

simplifying,

$$\Delta\ Vs\ =\ \frac{-\ M\ p^2\Delta\delta +\ S_3\ \Delta\ \delta}{P_3} \qquad (3.26b)$$

equation 3.26b can be rewritten as follows,

$$\Delta\ Vs\ =\ -D\ \Delta\delta \qquad (3.27)$$

where $$D\ =\ D_0 p^2 +\ D_1 p\ +\ D_2 \qquad (3.28a)$$

$$D_0 = \frac{M}{P_3} \qquad (3.28b)$$

$$D_1 = \ 0 \qquad (3.28c)$$

$$D_2 = \frac{S_3}{P_3} \qquad (3.28d)$$

subtituing 3.27 into 3.13

$$\Delta\ E_{qe}\ =\ \frac{AD}{B}\ \Delta\delta \qquad (3.29)$$

Equating 3.29 and 3.23,

$$\frac{-C\,\Delta\delta}{P_1} = \frac{AD}{B}\,\Delta\delta \qquad (3.30)$$

$$\Delta\delta\left(\frac{AD}{B} + \frac{BC}{P_1}\right) = 0 \qquad (3.30a)$$

$$ADP_1 + BC = 0 \qquad (3.30b)$$

which is the system performance equation.

Substituting the values of A, B, C and D into equation 3.30b, we obtain

$$A(D_0p^2 + D_1p + D_2)P_1 + (B_0p^2 + B_1p + B_2)$$
$$(C_0p^3 + C_1p^2 + C_2p) = 0 \qquad (3.31)$$

where,

$$AD_0p^2P_1 + AD_1pP_1 + AD_2P + B_0C_0p^5 +$$
$$B_0C_1p^4 + B_0C_2p^3 + B_0C_3p^2 + B_1C_0p^4 +$$
$$B_1C_1p^3 + B_1C_2p^2 + B_1C_3p + B_2C_0p +$$
$$B_1C_1p^2 + C_2B_2p + B_2C_3 \qquad (3.31a)$$

then, the following fifth order polynomial is obtained:

$$p^5\ (B_0C_0) + p^4\ (B_0C_1 + B_1C_0) + p^3\ (B_0C_2 + B_1C_1 + B_2C_0) + p^2\ (AD_0P_1 + B_0C_3 + B_1C_2 + B_2C_1) + p\ (B_1C_3 + B_2C_2) + (AD_2P_1+B_2C_3) = 0 \tag{3.32}$$

$$a_0p^5 + a_1p^4 + a_2p^3 + a_3p^2 + a_4p + a_5 = 0 \tag{3.33}$$

This is the fifth order polynomial of the investigated power system. The coefficients are a_0, a_1, a_2, a_3, a_4 and a_5 which are define as,

$$a_0 = C_0B_0 = \frac{T_{do}MP_1}{P_2}\ T_3T_e \tag{3.34}$$

$$a_1 = B_0C_1+B_1C_0 = (T_3T_e)M + (T_3+T_e)M\frac{T_{do}P_1}{P_2} \tag{3.35}$$

$$a_2 = B_0C_2 + B_1C_1 + B_2C_0 = (T_3T_e)\frac{(T_{do}P_1+S_2)}{P_2} + (T_3T_e)M + \frac{T_{do}MP_1}{P_2} \tag{3.36}$$

$$a_3 = AD_0P_1 + B_0C_3 + B_1C_2 + B_2C_1$$

$$= Kov M\frac{P_1}{P_3} + (T_3T_e)S_1 + (T_3+T_e)\left(T_{do}\frac{P_1}{P_2} + S_2\right) + M \qquad (3.37)$$

$$a_4 = AD_1P_1 + B_1C_3 + B_2C_2$$

$$= Kov(0)P_1 + (T_3+T_e)S_1 + T_{do}\frac{P_1}{P_2}S_2 \qquad (3.38)$$

$$a_5 = AD_2P_1 + B_2C_3 = Kov\ S_3\frac{P_1}{P_3} + S_1 \qquad (3.39)$$

It is to be noted here that parameter k_{ov} is the AER unknown gain parameter.Since stability results are sought in terms of this parameter, we would then re-arrenge equations 3.33 through 3.39 into the following form:

$$a_0p^5 + a_1p^4 + a_2p^3 + (KovZ_1 + \Delta A_3)p^2 +$$

$$(KovZ_2 + A_4)p + (KovZ_3 + \Delta A_5) = 0 \qquad (3.40)$$

where

$$Z_1 = \frac{MP_1}{P_3} \qquad (3.41a)$$

$$Z_2 = D_1 P_1 = 0 \qquad (3.41b)$$

$$Z_3 = \frac{S_3 P_1}{P_3} \qquad (3.41c)$$

$$\Delta A_3 = (T_3 T_e) S_1 + (T_3 + T_e)\left(T_{do} \frac{P_1}{P_2} + S_2\right) + M \qquad (3.41d)$$

$$\Delta A_4 = (T_3 + T_e) S_1 + T_{do} \frac{P_1 S_2}{P_2} \qquad (3.41e)$$

$$\Delta A_5 = S_1 \qquad (3.41f)$$

The power system performance shown in equation 3.40 is required in order to apply the frequency domain technique, which will be briefly describe in the next section.

3.4 *Frequency Domain Technique*

The numerical values of various coefficients of the performance equation (a_0, a_1, a_2, ...a_n) can be interpreted geometrically as a point in space having coordinates (a_0, a_1, a_2, ...a_n).

To each point in this space, it corresponds a definite set of coefficients (a_0, a_1, a_2,.......a_n) and consequently definite values of all roots (p_1, p_2, ...p_n). If in this space, there exists a region in which each point corresponds to a performance equation whose roots lie left of the imaginary axis in the complex plane (or p plane), then the profile bounding region (or locus) is called the boundary of stability.

Since all coefficients are functions of the system parameters, one can as well plot the region of stability in the parametric space. If there are only two parameters varying, the region of stability will be a plane. If there is only one varying parameter, the region will be a straight line. If any parameter varies continously, roots may then cross over to the right half plane or from right to left half plane, then the boundary of the region of stability can be thought as a reflection of the imaginary axis of the root plane. This suggest a procedure for constracting the stability locus.

3.4.1 *Construction of Stability Locus.- in the Plane of Parameter* k_{OV}

A performance equation can be arranged as follows:

$$S(p) + K\,Q(p) = 0 \tag{3.42}$$

where K is a complex unknown variable. S(p) are the terms in the performance equation which are not associated with K. Q(p) are the terms associated with K.

Replacing "p" by jw in equation 3.42,we obtain,

$$S(jw) + K\,Q(jw) = 0 \tag{3.43}$$

solving for k,

$$K = \frac{-S(jw)}{Q(jw)} = Re\,(K) + jIm(K) \tag{3.44}$$

"W" can be assumed to have a range from $-\infty$ *to* $+\infty$*. Substituting these values into equation 3.44, a locus for K can be obtained. After this locus is developed in the complex plane of K, the Routh-Hurwitz [20] criterion can be applied to check for stability.*

3.4.2 *Application of the Frequency Domain Technique to the System Under Investigation*

Equation 3.40, which is the performance equation can be rearranged as,

$$Kov(Z_1p^2 + Z_2p + Z_3) + (a_0p^5 + a_1p^4$$

$$+ a_2p^3 \quad + \Delta A_3p^2 + \Delta A_4p + \Delta A_5) = 0 \qquad (3.45)$$

comparing with equation 3.42, we obtain

$$Q(p) = Z_1p^2 + Z_2p + Z_3 \qquad (3.46)$$

and

$$P(p) = a_0p^5 + a_1p^4 + a_2p^3 + \Delta A_3p^2 + \Delta A_4p + \Delta A_5 \qquad (3.47)$$

replacing p by jw in equations 3.46 and 3.47, and the separating the real and imaginary parts, we obtain

$$P(jw) = P_{real} + jP_{imag} = P_{11} + jP_{22} \qquad (3.48)$$

$$Q(jw) = Q_{real} + jQ_{imag} = Q_{11} + jQ_{22} \qquad (3.49)$$

then substituing the above equations into 3.44,we obtain

$$Kov = \frac{-(P_{11} + jP_{22})}{(Q_{11} + jQ_{22})} = Re(K_{ov}) + jIm(K_{ov}) \qquad (3.50)$$

where

$$Re(K_{ov}) = \frac{- P_{11}Q_{11} + P_{22}Q_{22}}{Q_{11}^2 + Q_{22}^2} \qquad (3.51)$$

$$Im(K_{ov}) = \frac{- P_{22}Q_{11} + P_{11}Q_{22}}{Q_{11}^2 + Q_{22}^2} \qquad (3.52)$$

From equations 3.51 and 3.52, the stability locus can then be plotted on the two-dimensional real-imaginary plane of K_{ov} *for any operating condition.*

For the system studied P_{11}, P_{22}, Q_{11} *and* Q_{22} *are defined as follows,*

$$P_{11} = (a_1w^4 - \Delta A_3w^2 + \Delta A_5) \qquad (3.53)$$

$$P_{22} = j(a_0w^5 - a_2w^3 + \Delta A_4w) \qquad (3.54)$$

$$Q_{11} = Z_1w^2 + Z_3 \qquad (3.55)$$

$$Q_{22} = j(Z_2w) \qquad (3.56)$$

3.5 *Computer Simulation.-*

Examining the terms P_{11}, P_{22}, Q_{11} and Q_{22} it is clear that these are functions of the power derivatives P_1,S_1, P_2, S_2, P_3 and S_3 and of other system parameters. The values of the above terms vary from one operation condition to another. The following strategy for algorithms development is suggested :

Step #1- Obtain overall generalized circuit constants A_0, B_0, C_0 and D_0 of the transmission network under study.

Step #2- Construct the active and reactive power values of the generator bus.

Step #3- Using the results of step #2 evaluate the generator internal voltages and angles.

Step #4- Using the results of steps 2 and 3 compute the power derivatives for the network at any given operating condition.

Step #5- *Using the results of step #4, the terms* P_{11}, P_{22}, Q_{11} *and* Q_{22}*can be estimated and later used do defined the stability locus.*

A computer simulation program was developed to solve steps 1 through 5 . A flowchart for this program is shown in figure 11 below,

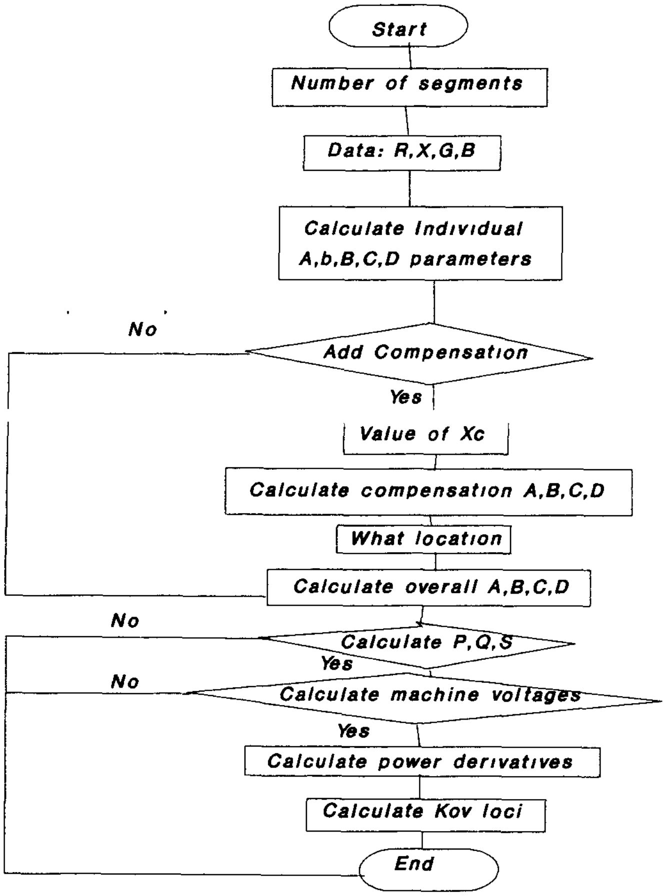

Figure 11

Then the Routh-Hurwitz (R-H) criteria was applied to determine which side of stability locus is stable, table 3.1 below was developed to apply the R-H criteria ,

TABLE 3.1

Routh Array

	$a0$ $a1$	$a2$ $a3$	$a4$ $a5$
$\lambda_1 = \frac{a0}{a1}$	$C13 = \frac{a1\,a2 - a0\,a3}{a1}$	$C23 = \frac{a1\,a4 - a0\,a5}{a1}$	$C33 = 0$
$\lambda_2 = \frac{a1}{C13}$	$C14 = \frac{C13\,a3 - C23\,a1}{C13}$	$C24 = \frac{C13\,a3 - a1\,C33}{C13}$	
$\lambda_3 = \frac{C13}{C14}$	$C15 = \frac{C23\,C14 - C13\,C24}{C14}$	$C25 = 0$	
$\lambda_4 = \frac{C14}{C15}$	$C16 = \frac{C24\,C15 - C14\,C25}{C15}$		

CHAPTER IV

4.1 Computation of Generalized Circuit Constants.-

A transmission line is modelled as the π network shown in figure 12.a. This network can be expressed in terms of its generalized circuit constants as shown in figure 12.b.

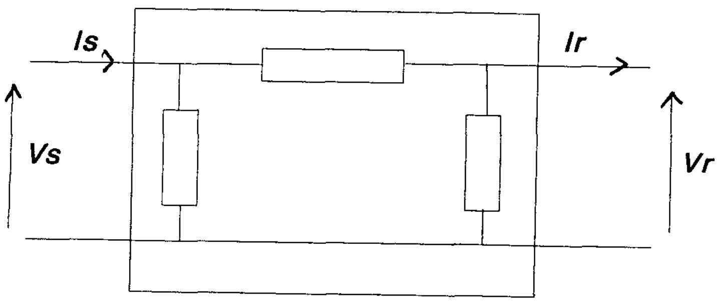

Figure 12.a

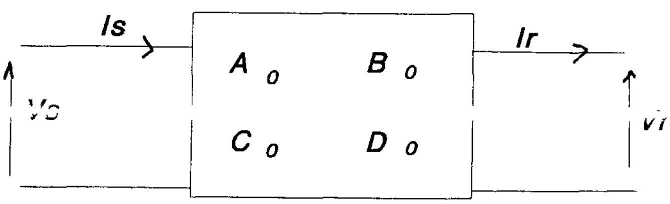

Figure 12.b

$$V_s = AV_r + BI_r \tag{4.1}$$

$$I_s = CV_r + DI_r \tag{4.2}$$

Where constants A, B, C and D parameters are defined as:

$$A = 1 + \frac{ZY}{2} \tag{4.3a}$$

$$B = Z \tag{4.3b}$$

$$C = Y + \frac{Y^2 Z}{4} \tag{4.3c}$$

$$D = \frac{ZY}{2} + 1 = A \tag{4.3d}$$

Equations 4.1 and 4.2 can also be represented in matrix form:

$$\begin{vmatrix} V_s \\ \\ I_s \end{vmatrix} = \begin{vmatrix} A & B \\ \\ C & D \end{vmatrix} \begin{vmatrix} V_r \\ \\ I_r \end{vmatrix} \tag{4.4}$$

Likewise a series capacitor can be represented in the matrix form. Refering to figure 13, the following generalized circuit constants are defined for a series capacitor:

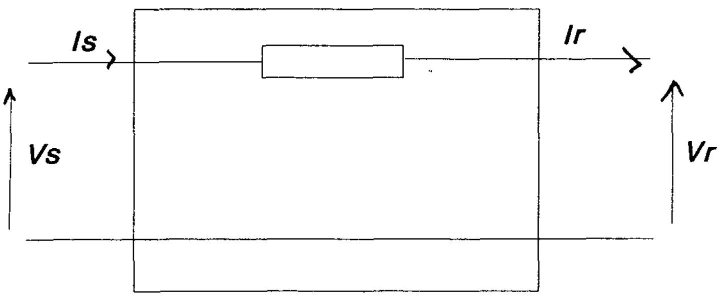

Figure 13

$$V_1 = V_2 + Z\, I_2 \qquad (4.5)$$

$$I_1 = 0\, V_2 + I_2 \qquad (4.6)$$

where,

$$A = 1 \qquad (4.7a)$$

$$B = Z = -X_c \qquad (4.7b)$$

$$C = 0 \qquad (4.7c)$$

$$D = 1 \qquad (4.7d)$$

4.2 Determination of the Overall Constants Ao, Bo, Co and Do

For the system studied, the system had to be modelled in terms of its overall circuit constants. As it was indicated in chapter 3 a computer algorithm was developed to compute the overall circuit constans. The base case was the existing uncompensated case.

<u>Case 1, Uncompensated Power Network</u>; The existing Power network (figure 1) was simplified to one machine representationas as shown below in figure 14.a. Segment 1 represents the the equivalent impedance of the network between the 765 kV Chataguey bus and the Beauharnois generators, these segment include step-up transformers. Segment 2 represents the MSC-7040 line and Segment 3 the MSU-1 line. The computer program will first determine the A, B, C, and D constants of each segment, figure 14.b. Then these segments are combined to obtain the overall A_O, B_O, C_O *and* D_O *equivalent, figure 14.c.*

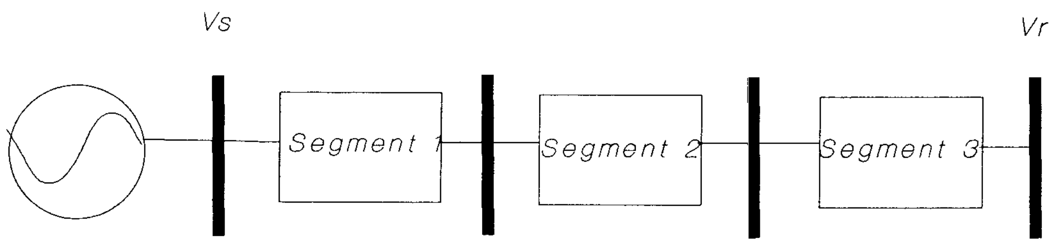

Figure 14.a

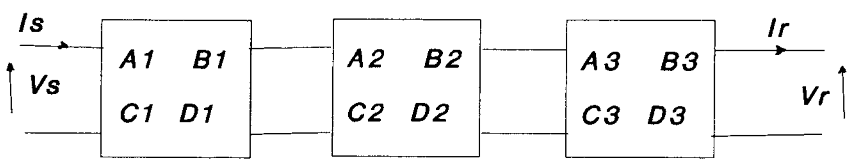

Figure 14.b

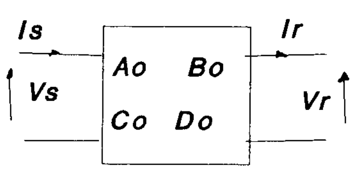

Figure 14.c

The MSU-1 line, MSC-7040 and the equivalent network line parameters are given in pu quantities, with a 100 MVA base,in Appendix A.

<u>Case 2: 20% Self Compensation of the MSU-1 line at the source side</u>;The power network of case 1, was then modified for compensation of the MSU-1 line, placing the compensation at the source side of the line. This network is shown in figure 15.a below. The computer program calculated the new overall circuit constants, A'_O, B'_O, C'_O and D'_O by modifiying the circuit of case 1 to place the the circuit constants of the series capacitor in the proper location of the modified array. Figure 15.b shows the new overall block diagram for case 2.

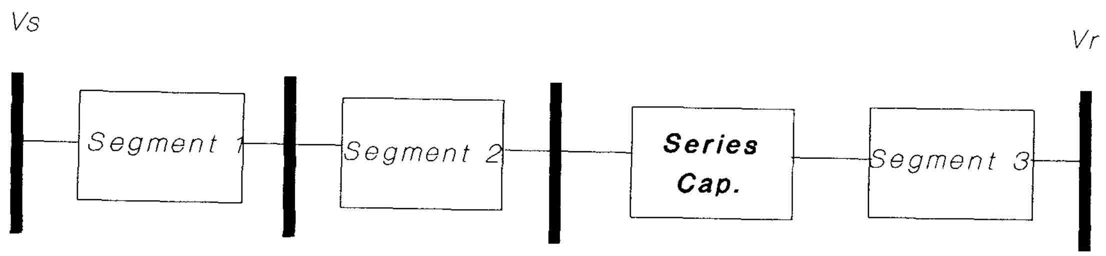

Figure 15.a

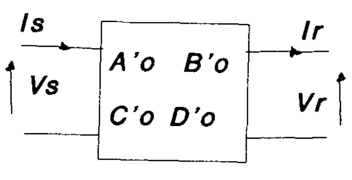

Figure 15.b

<u>Case 3: 20% self Compensation of the MSU-line at the Load Side;</u> *Similarly to case 2, the original uncompensted network of case 1 was modified to place compensation at the load side of the MSU-1 line. The same procedure perform by the computer program in case 2 was done here to place the circuit constants of the series compensation in the proper order of the modified array. Again new overall circuit constants* A'_o, B'_o, C'_o *and* D'_o *were determined for this case. Figures 16.a and 16.b show the modified network and the new overall block diagram.*

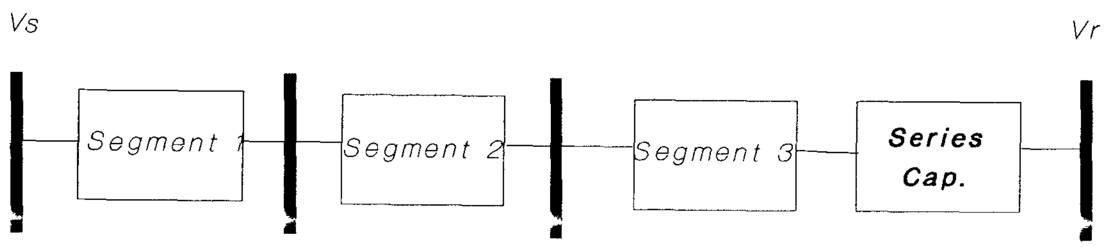

Figure 16.a

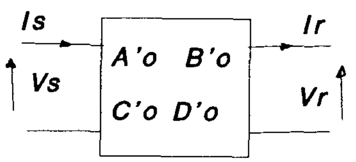

Figure 16.b

Case 4: 20% self Compensation of the MSU-line at Both Ends; The 20% compensation was divided in half and placed at both ends of the MSU-1 line. The same procedure outline for the above cases was performed by the computer program. Figures 17.a and 17.b show the modified network and the new overall block diagram.

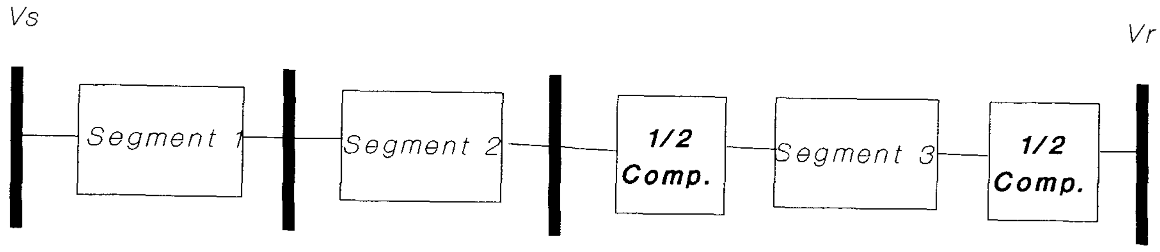

Figure 17.a

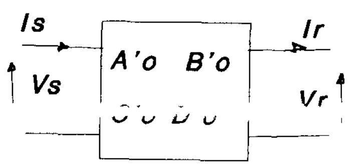

Figure 17.b

Case 5: 20% self Compensation of the MSU-line Place at the Midle of the Line; This time the compensation was placed in the middle of the line. For this case the computer program first models the MSU-1 line as two segments by recalculating the circuit constants and then places the series capacitor circuit constants in the proper array location. Figures 18.a and 18.b show the modified network and the new overall block diagram.

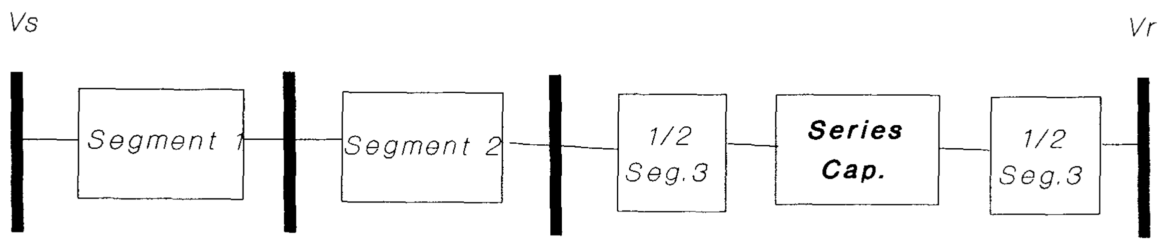

Figure 18.a

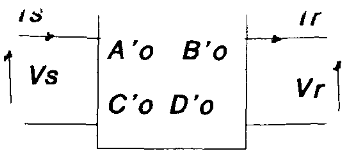

Figure 18.b

A similarly procedure of series compensation was performed for the MSC-7040 line as for the MSU-1 line. The MSC-7040 was compensated witn 20% of its line reactance and the same locations as for the MSU-1 line were tested in the MSC-7040 line. These cases are:

<u>Case 6:</u> 20% Self Compensation of the MSC-7040 line at the source side. Figures 19.a and 19.b show this case.

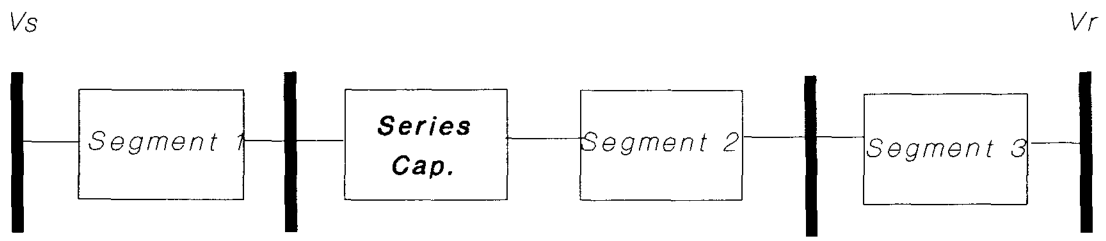

Figure 19.a

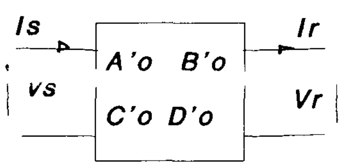

Figure 19.b

<u>Case 7:</u> 20% self Compensation of the MSC-7040 line at the load side. Figures 20.a and 20.b show this case.

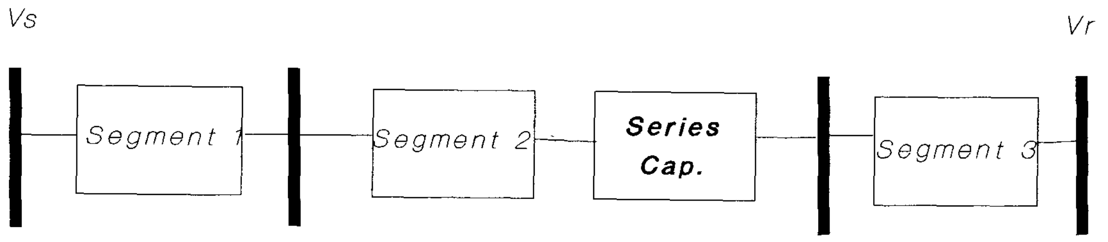

Figure 20.a

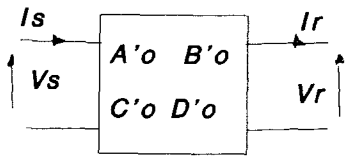

Figure 20.b

Case 8: *20% self Compensation of the MSC-7040 line at both ends. Figuresw 21.a and 21.b show this case.*

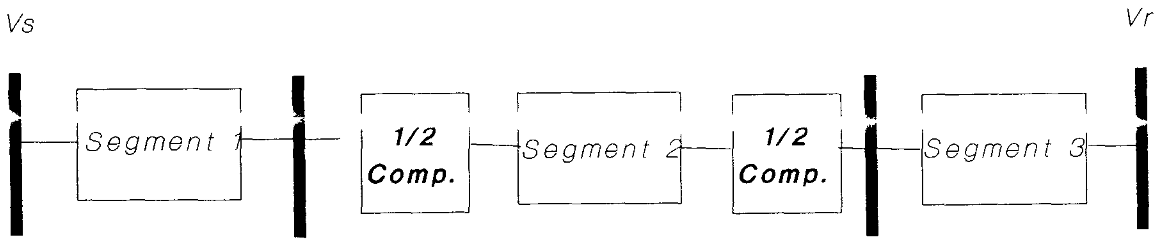

Figure 21.a

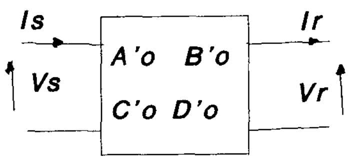

Figure 21.b

Case 9: 20% self Compensation of the MSC-7040 line, place at the midle of the line. Figures 22.a and 22.b show this case.

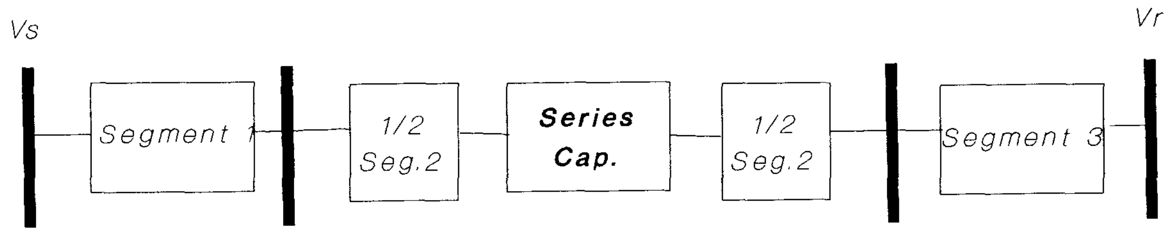

Figure 22.a

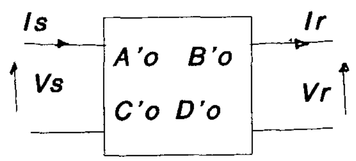

Figure 22.b

Case 10: Finally compensation was added at the physical center of the MSU-1 and MSC-7040 lines. The network diagram was modified to shown this new location. Figures 23.a and 23.b show

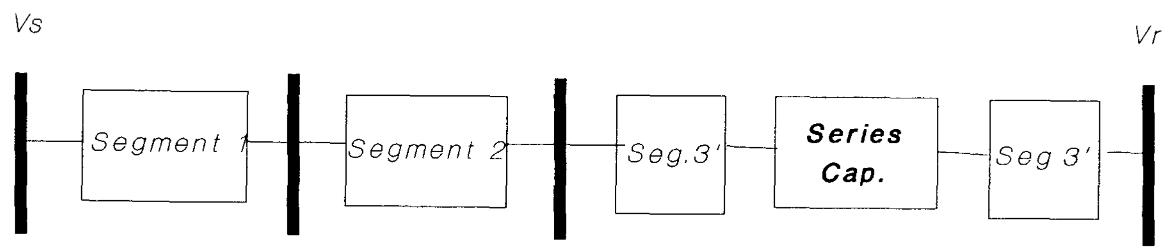

Figure 23.a

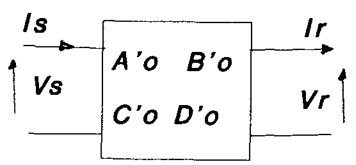

Figure 23.b

4.3 Computation of Active and Reactive Power Characteristics.-

Equations 4.1 and 4.2 can be rewritten with the overall constants A_o, B_o, C_o and D_o which were previously determine for each case described in the previous section, as shown below,

$$V_s = AoV_r + BoI_r \tag{4.8}$$

$$I_s = CoV_r + DoI_r \tag{4.9}$$

from equation 4.8, we get

$$I_r = \frac{V_s - AoV_r}{Bo} \tag{4.10}$$

Substituting 4.10 into 4.9

$$I_s = CoV_r + \frac{Do(V_s - AoV_r)}{Bo} \tag{4.11}$$

$$I_s = \frac{D}{B}V_s + [C - A\frac{D}{B}]V_r \tag{4.11a}$$

Let $Vr = Vr \angle\theta$ and $Vs = Vs \angle \theta = Vs(\cos \theta + j\sin \theta)$. Then,

$$I_s = \frac{D(\cos\theta + j\sin\theta)}{B} + \frac{[C - AD]V_r}{B} \qquad (4.11b)$$

The apparent power of the network is

$$S = V_s\, I_s^{*} \qquad (4.12)$$

$$S = V_s(\cos\theta + j\sin\theta)\left[\frac{D^{*}V_s(\cos\theta - j\sin\theta)}{B^{*}} + \frac{[C^{*} - A^{*}D^{*}]V_r}{B^{*}}\right] \qquad (4.13)$$

After simplifying and rearranging equation 4.13, we obtain:

$$S_s = P_s + jQ = \qquad (4.14)$$

$$S_s = |S_s| \angle \theta_s = \sqrt{P^2 + Q^2}\ \angle \tan^{-1} \frac{Q_s}{P_s} \qquad (4.15)$$

where,

$$P_S = V_S\left[\frac{DV_S\cos\psi_1}{B} + \left(C\cos(-\theta_C) - \frac{AD\cos{}_2}{B}\right)\cos\theta + \left(\frac{AD\sin\psi_2}{B} - C\sin(-\theta_C)\right)\sin\theta\right] \tag{4.16}$$

$$Q_S = V_S\left[\frac{DV_S\sin\psi_1}{B} + \left(C\sin(-\theta_C) - \frac{AD\sin\psi_2}{B}\right)\cos\theta + \left(\frac{AD\cos\psi_2}{B} - C\cos(-\theta_C)\right)\sin\theta\right] \tag{4.17}$$

where

$$\psi_1 = -\theta_D + \theta_B$$

$$\psi_2 = -\theta_A + \psi_1$$

also

also	$A = A\angle\theta_A$	$A^{*} = A\angle-\theta_A$
	$B = B\angle\theta_B$	$B^{*} = B\angle-\theta_B$
	$C = C\angle\theta_C$	$C^{*} = C\angle-\theta_C$
	$D = D\angle\theta_D$	$D^{*} = D\angle-\theta_D$

From equations 4.16 and 4.17 the active and reactive power values at the generator bus can be obtainaed for any operating condition θ.

The results for the active and reactive power characteristics for the uncompensated case and for each compensated cases are shown in figures 24 through 26.d for 20% compensation of its own line impedance. Each figure also shows the power characteristics for the source voltage, Vs, at 1.0 and 1.05 pu with the receiving end voltage mantain at 1.0 pu for both cases.

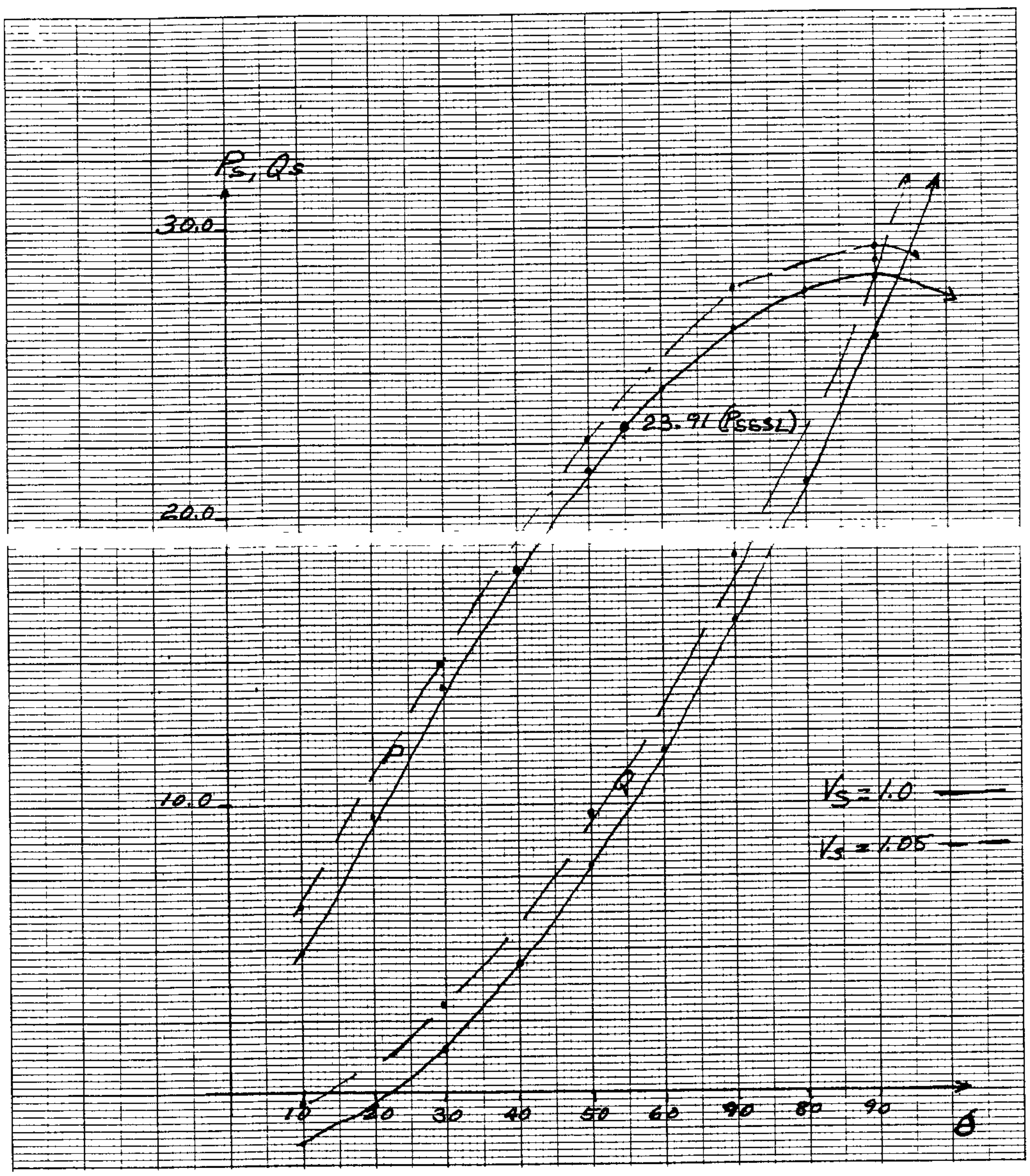

Figure 24

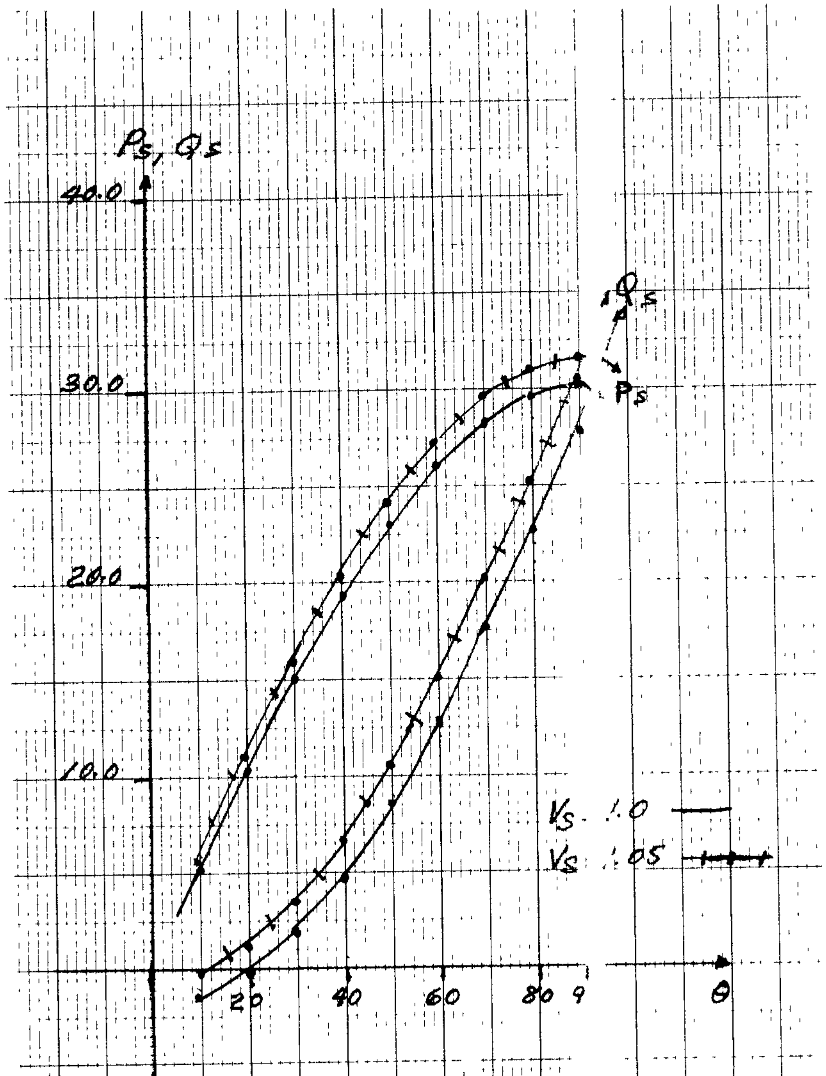

Figure 25.a

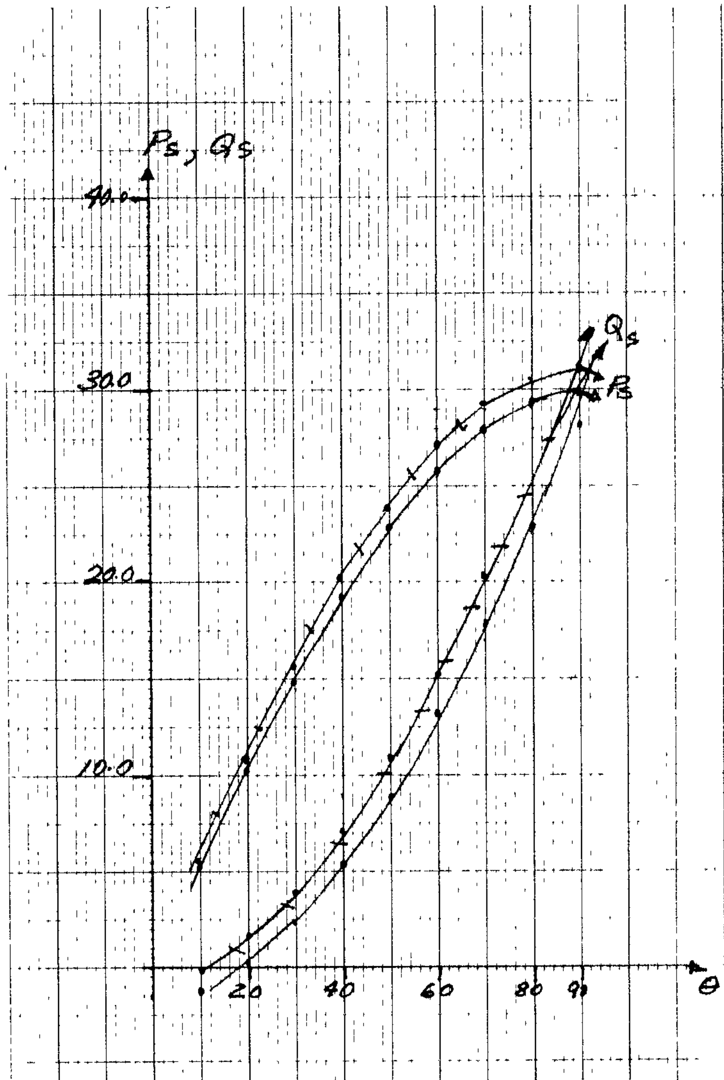

Figure 25.b

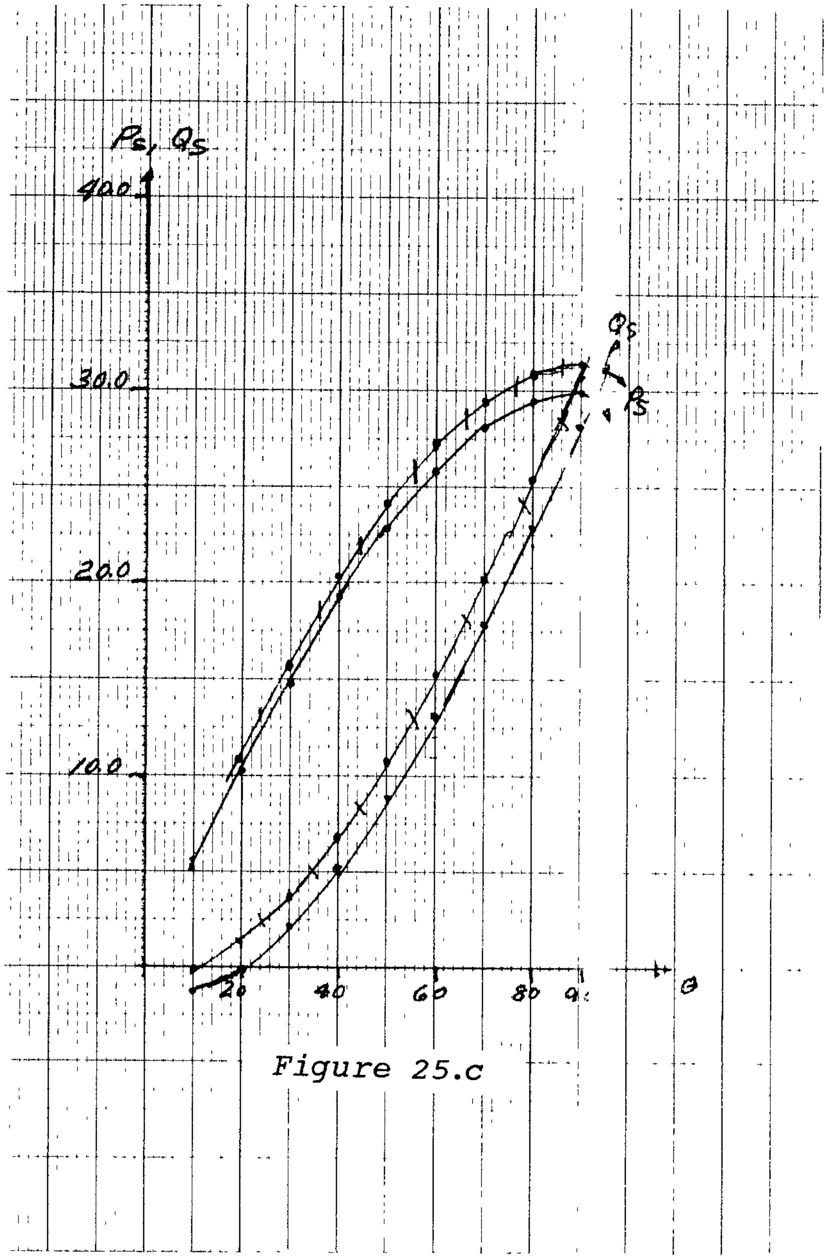

Figure 25.c

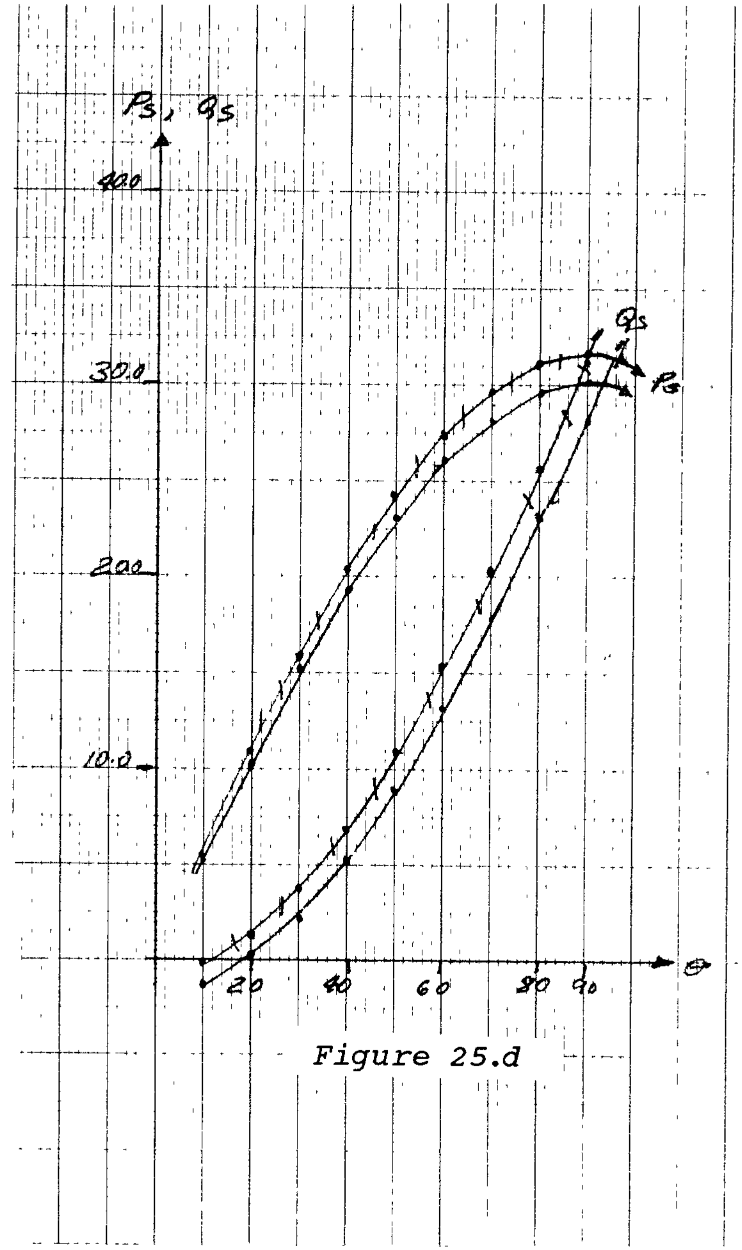

Figure 25.d

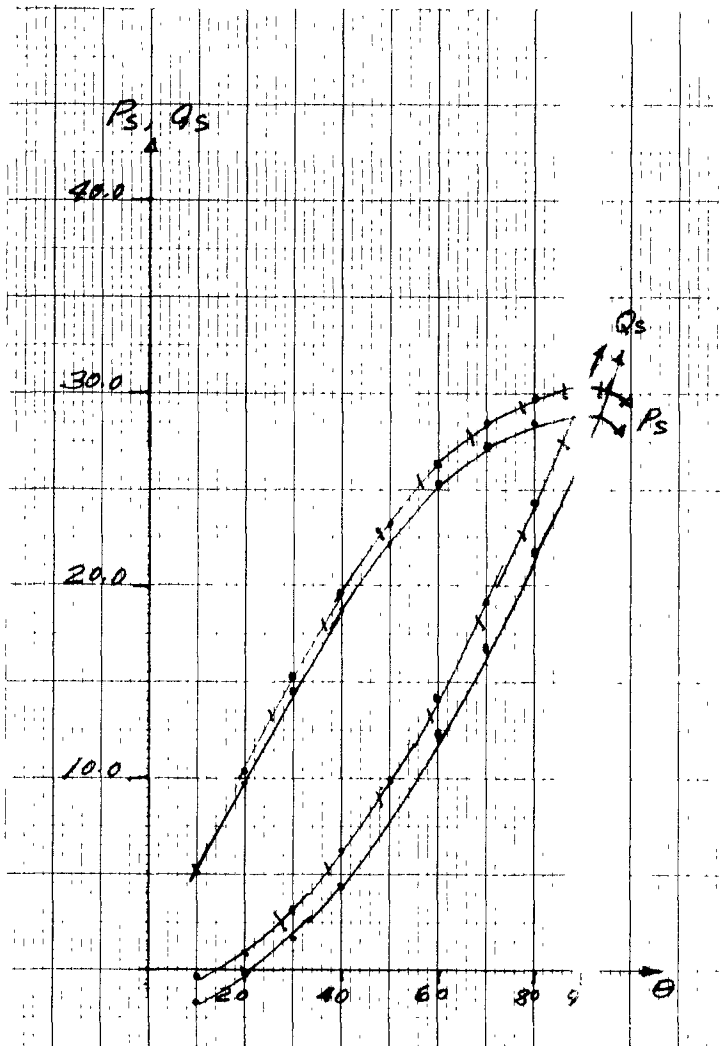

Figure 26.a

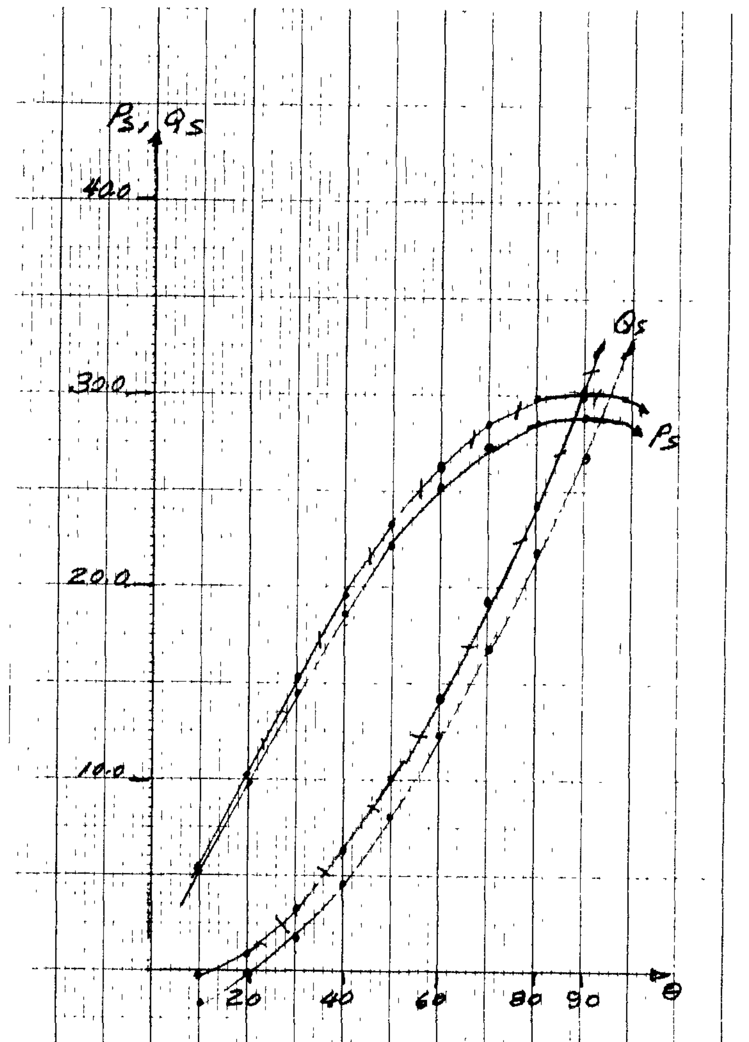

Figure 26.b

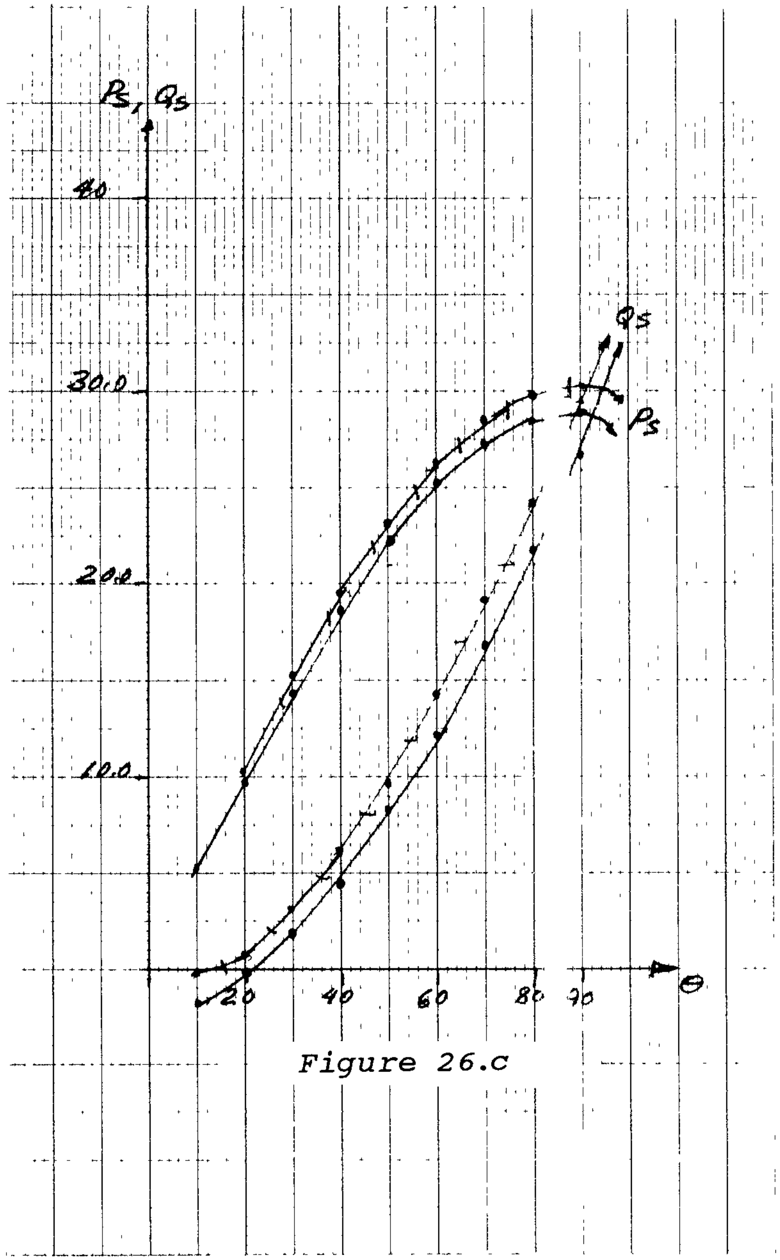

Figure 26.c

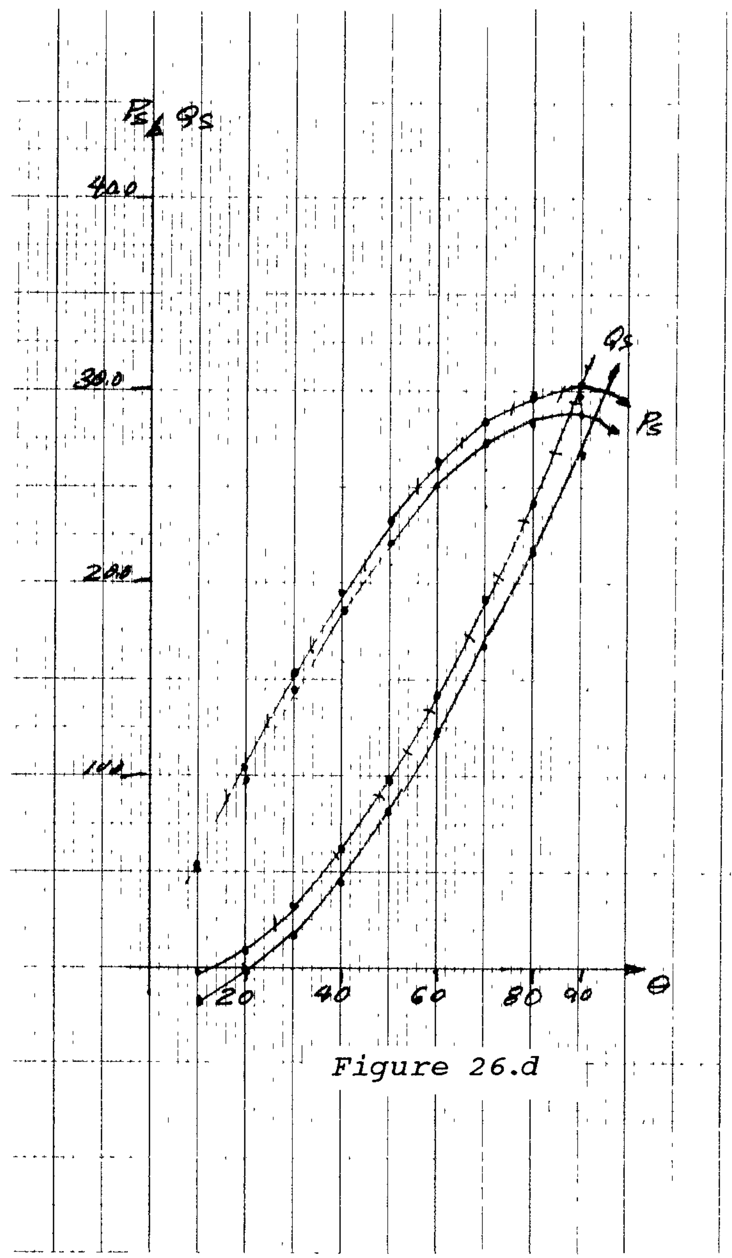

Figure 26.d

4.4 Computation of Generator Internal Voltage Angles.-

Referring to the phasor diagram, figure 10, of a salient pole synchronous machine, various internal voltages behind the synchronous reactance and internal torque angles in terms of active and reactive power flows can be determined for any operating condition.

The open circuit voltage is:

$$E_q = \sqrt{\left(V_s + \frac{x_q\ Q_s}{V_s}\right)^2 + \left(\frac{P_s\ x_q}{V_s}\right)^2} \qquad (4.18)$$

$$\delta_g = \arctan \frac{P_s\ x_q}{V_s^2 + x_q Q_s} \qquad (4.19)$$

The transient emf voltage is:

$$E' = \sqrt{\left(V_s + \frac{Q_s x_d'}{V_s}\right)^2 + \left(\frac{P_s x_d'}{V_s}\right)^2} \qquad (4.20)$$

$$\delta' = \arctan \frac{P_s\ x_q}{V_s + x_d' Q_s} \qquad (4.21)$$

The emf voltage proportional to the direction is:

$$E_q' = E' \cos(\delta g - \delta') \qquad (4.22)$$

then,

$$E_q = E_q \frac{x_d - x_d'}{x_q - x_d} - E_q \frac{x_d - x_q}{x_q - x_d} \qquad (4.23)$$

where x_d, x_d' and x_q are the unsaturated reactances of the hydro generator.

The details of H-Q equivalent generator unsaturated reactances are given on Appendix I.

4.5 Computation of Power Derivatives.-

The power derivatives equations P_1, S_1, P_2, S_2, and P_3, S_3 can be derived from the phasor diagram figure 10, by defining the power output expressions.

$$P_{Eq} = \frac{E_q V}{x_{d\Sigma}} \sin \delta + \frac{V^2}{2} \frac{x_d - x_q}{x_{q\Sigma} x_{d\Sigma}} \sin 2\delta \qquad (4.24)$$

$$P_{Eq}' = \frac{E_q' V}{x_{d\Sigma}'} \sin \delta + \frac{V^2}{2} \frac{x_q - x_d'}{x_{q\Sigma} x_{d\Sigma}} \sin 2\delta \qquad (4.25)$$

$$PV_{gq} = \frac{V_{gq}V}{x_e} \sin\delta + \frac{V^2}{2} \frac{x_q}{x_q \quad x_e} \sin 2\delta$$

(4.26)

$$PV_g = \frac{V_r V_g}{x_e} \cos g \sin\delta + \frac{V^2}{2} \frac{x_q}{x_q \; x_e} \sin 2\delta$$

(4.27)

then from equations 3.7 through 3.12, the following expresions for the power derivatives can be obtained:

$$P_1 = \frac{V}{x_{d\Sigma}} \sin\delta$$

(4.28)

$$S_1 = \frac{E_q V}{x_{d\Sigma}} \cos\delta + V^2 \frac{x_d - x_q}{x_{q\Sigma} x_{d\Sigma}} \cos 2\delta$$

(4.29)

$$P_2 = \frac{V}{x_{d'\Sigma}} \sin\delta$$

(4.30)

$$S_2 = \frac{E_q' V}{x_{d'\Sigma}} \cos\delta - V^2 \frac{x_q - x_d'}{x_{q\Sigma} x_{d'\Sigma}} \cos 2\delta$$

(4.31)

$$P_3 = \frac{V}{x_e} \sin\delta \frac{1}{\cos\delta_g}$$ (4.32)

$$S_3 = \frac{V_g\ V}{x_e}\left(\cos\delta_g\ \cos\delta - \frac{1}{2}\sin\delta\ \frac{\sin 2\delta}{\cos\delta_g}\left(\frac{V\ x_g}{V_g x_q}\right)^2\right. \tag{4.33}$$

where

$$x_{d\Sigma} = x_d + x_e$$

$$x_{d'\Sigma} = x_d' + x_e$$

$$x_{q\Sigma} = x_q + x_e$$

x_e *is the transfer reactance of the power network between the generating point and the receiving end.*

The results of the machine internal voltages and angles and power derivatives, at different operating conditions, where the not included here for simplicity.

4.6 The Routh-Hurwitz Stability Criterion

The Routh-Hurwitz (R-H) test is used to determine stability for a time invariant,continuous system like the power system [20]. The R-H method tests the coefficients of the characteristic equation of a system. For the characteristic equation 3.27b

$$a_0p^5 + a_1p^4 + a_2p^3 + a_3p^2 + a_4p + a_5 = 0$$

the basic problem is to determine, without factoring p, whether all the roots of the characteristic equation lie in the left of the plane.The R-H test is done by creating the Routh array, shown in Table 3.1

The coefficients on the first column of the Routh array must be equal or greater than zero, To satisfy the R-H criteria.

CHAPTER V

Results and Discussions

5.1 Procedure on Actual Power Stability Limits for a System Employing IEEE Type I Excitation Control System;

The power system described in figure 1 was first symplified by finding the equivalent impedance between the Chataguay 765 kV bus and the Beahournois low side of the generator step-up transformers. The individual transformers and line impedances of the symplified section were first converted into a common base of 1000 MVA. The networks equivalent impedance was used as the line parameters for segment 1. Transformer losses were ignored.

The line parameters of the MSU-1 and MSC-7040 765 kV lines were converted to a 100 MVA base. Once all the network impedances were obtain they were input in the computer program as the base case study. The individuall A, B, C and D constants were obtained and then the overall circuit constants were calculated. The active and reactive power for any operating condition was then calculated. In this analysis the angle 0 between the generator and the infinite bus is defined as the operating condition. The result of this calculation was shown in the power angle curve of figure 24.

To obtain the stability locus the generator and exciter parameters were lumped toguether in order to symplified the modelling from thirtysix machines to an equivalent single machine. The direct-synchronous reactance, transient reactance and quadrature reactance (x_d, x'_d and x_q respectavily) of each generator was first converted into the common 100 MVA base. The equivalent reactances were then found by paralleling the impendances. The exciter time constants T_3 and T_e of the machines were averaged to obtained an equivalent constant. The equivalent generator field constant (T_{do}) was also obtained by averaging the thirty six time constants

The stability loci for diferent operating conditions was then determined and the stability region was determine by using the Routh-Hurwitz criteria. From this test the power steady state stability limit, P_{SSSL}, was determined to be 23.10 p.u. The maximum power transfer, Pmax, for this uncompensated case was determined to be 28.19 p.u.

Figures 27.a through 27.h show the stability loci for 20, 30, 40, 50, 54, 55, 56 and 60 degrees, with 55 degrees as the P_{SSSL}.

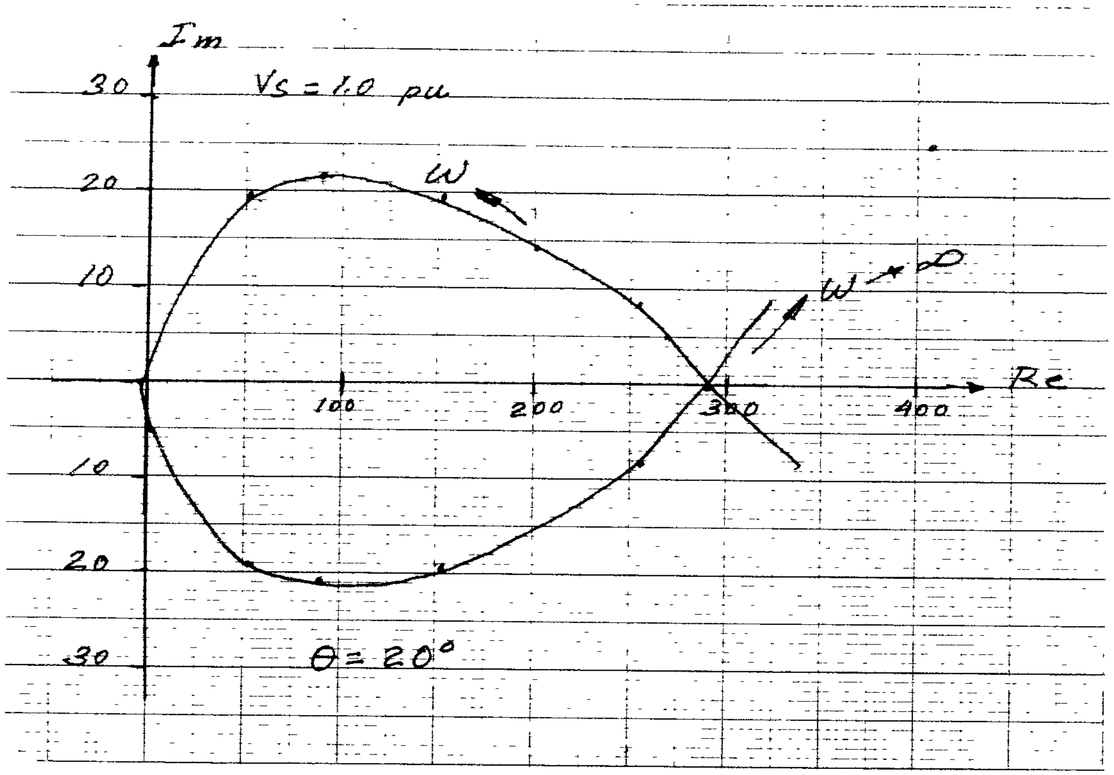

Figure 27.a

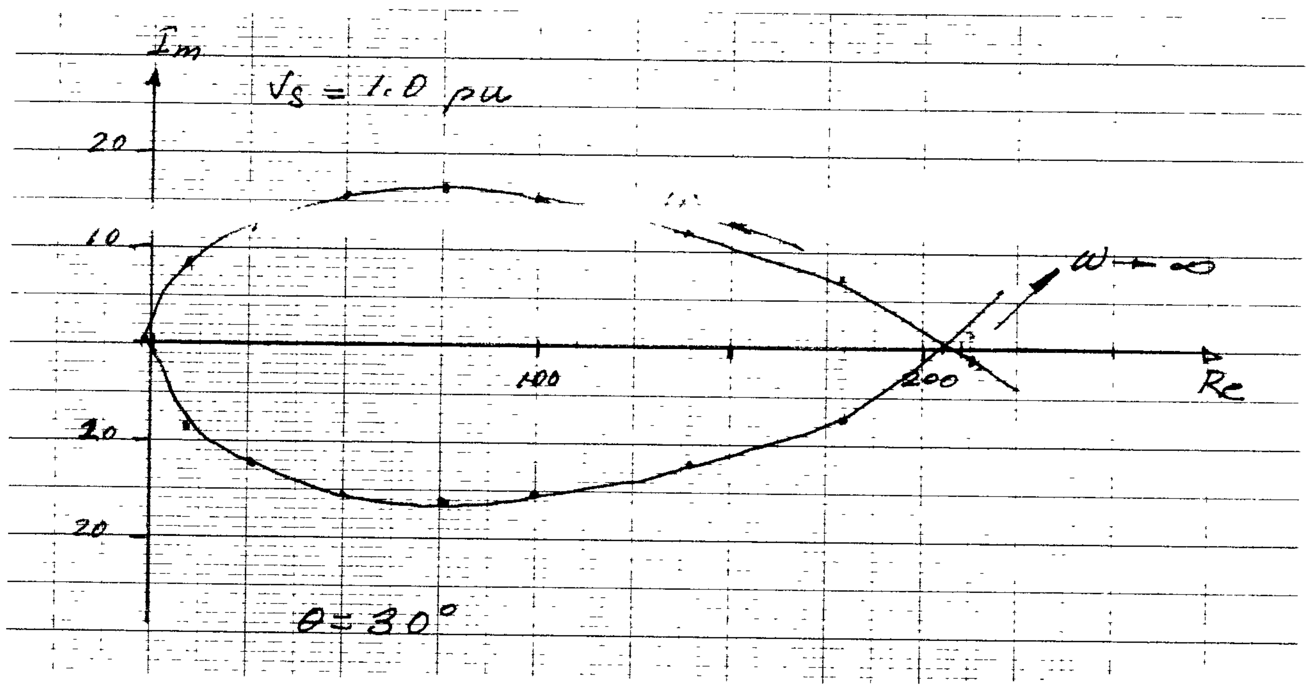

Figure 27.b

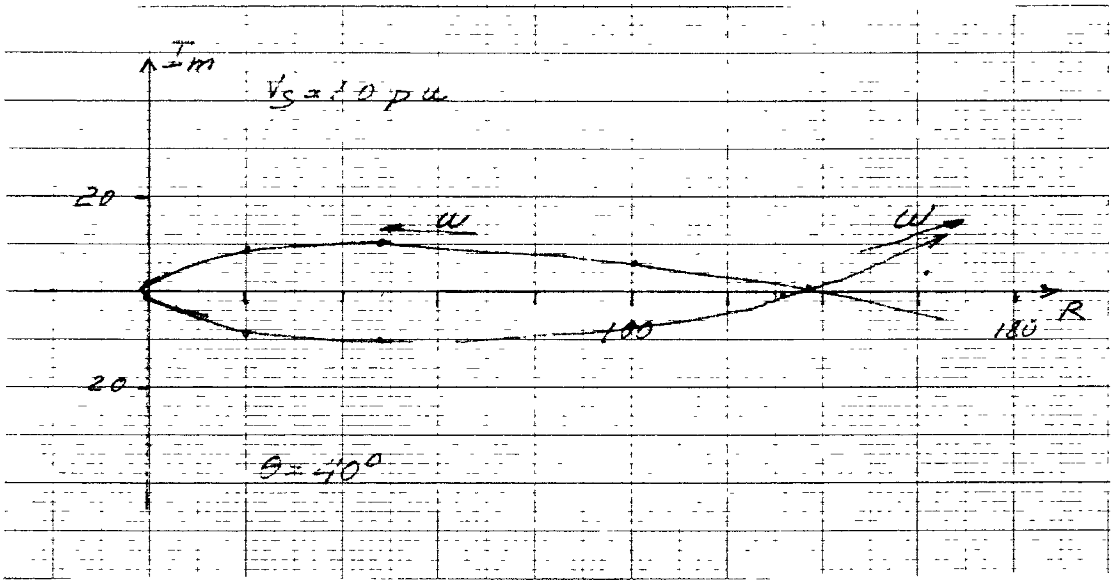

Figure 27.c

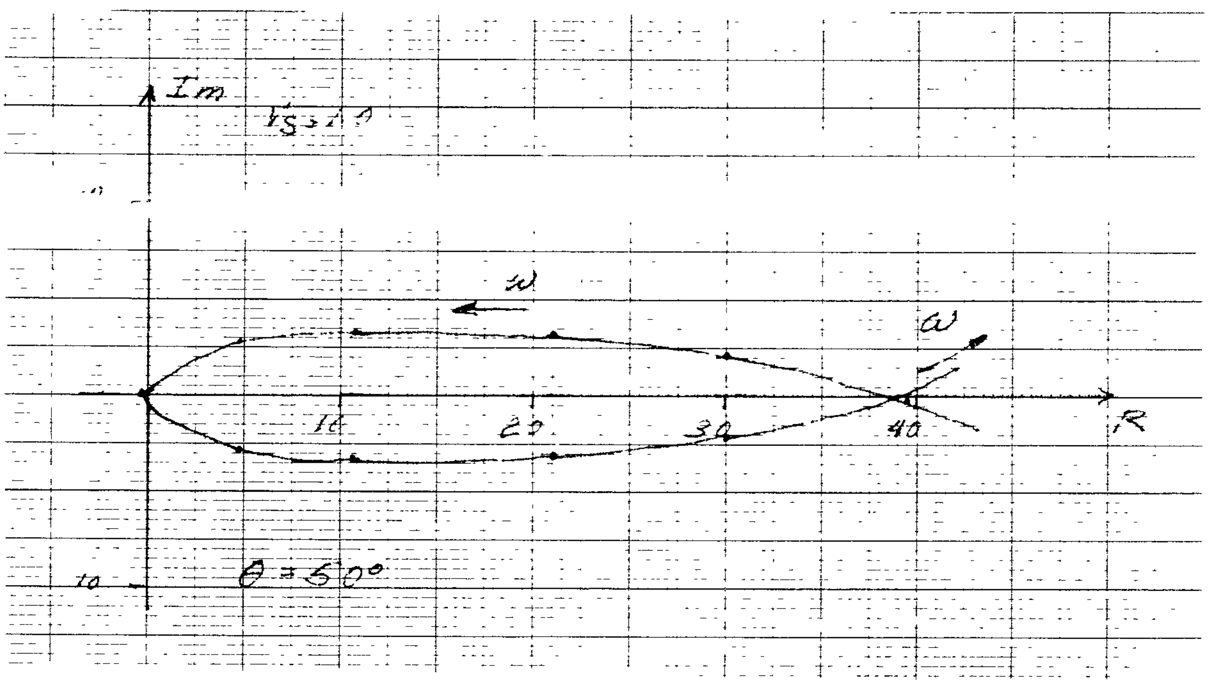

Figure 27.d

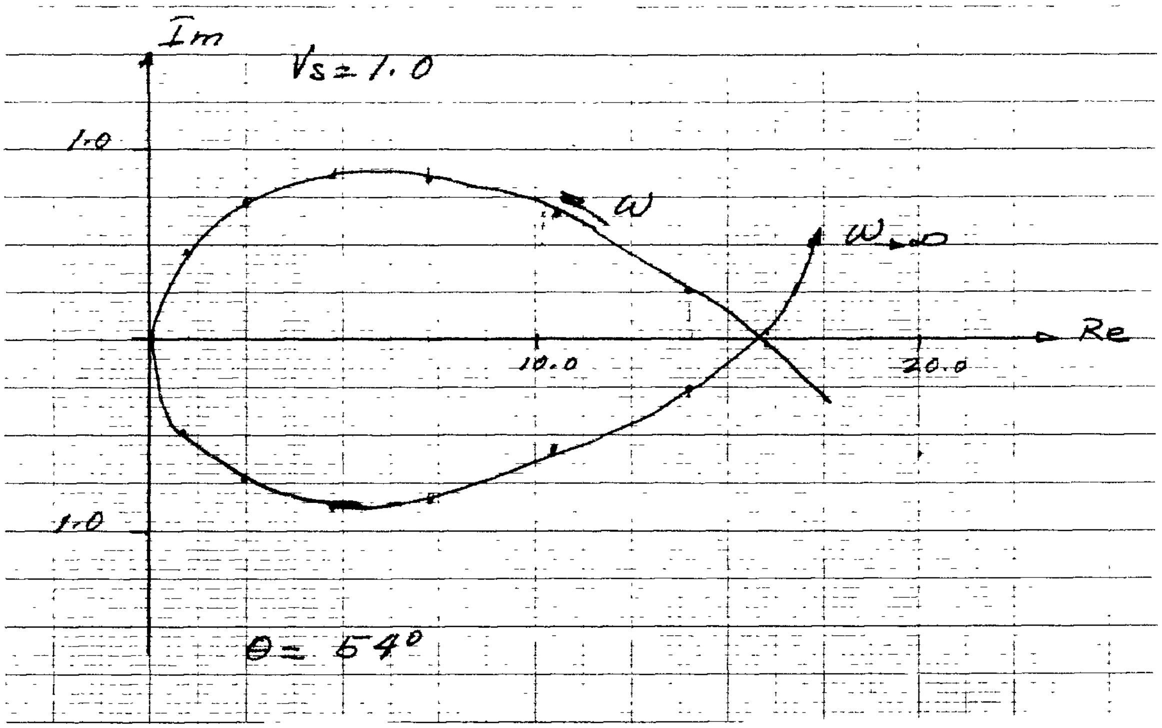

Figure 27.e

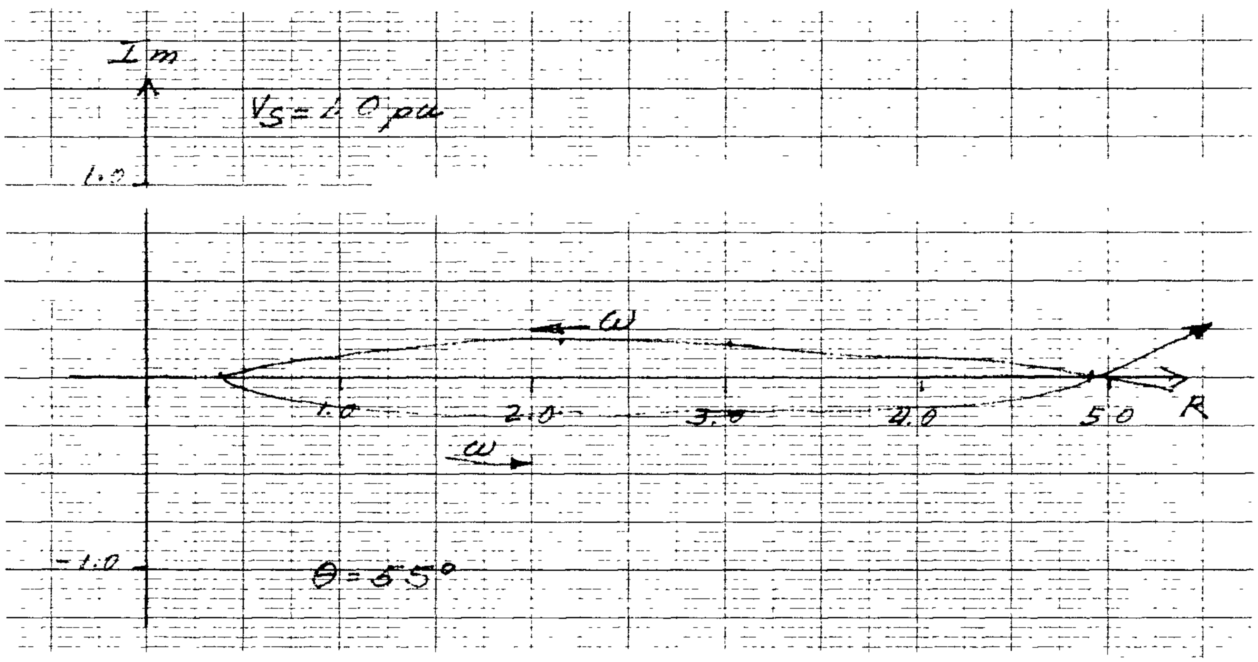

Figure 27.f

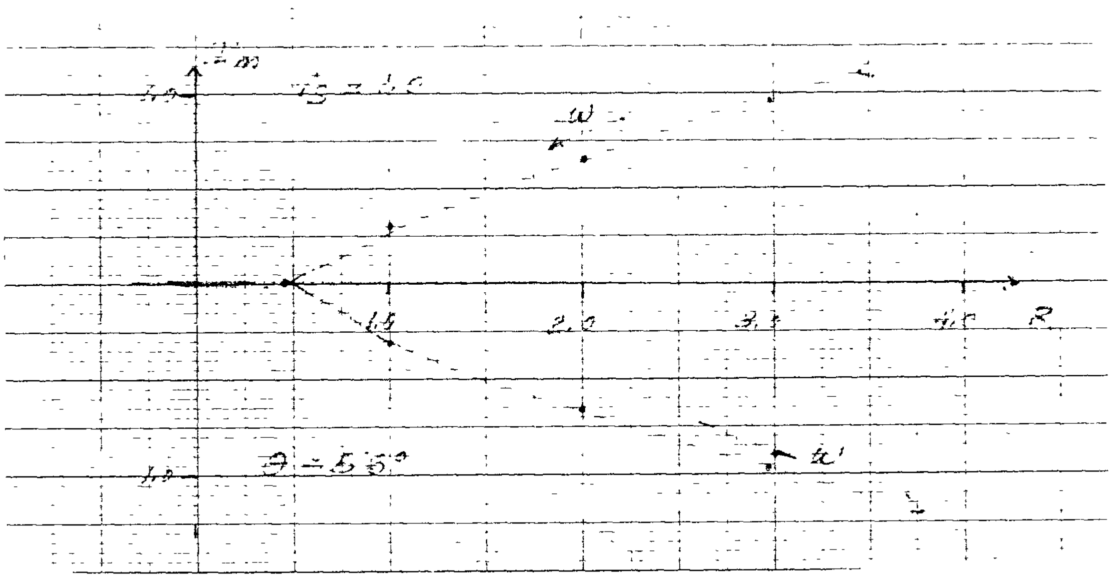

Figure 27.g

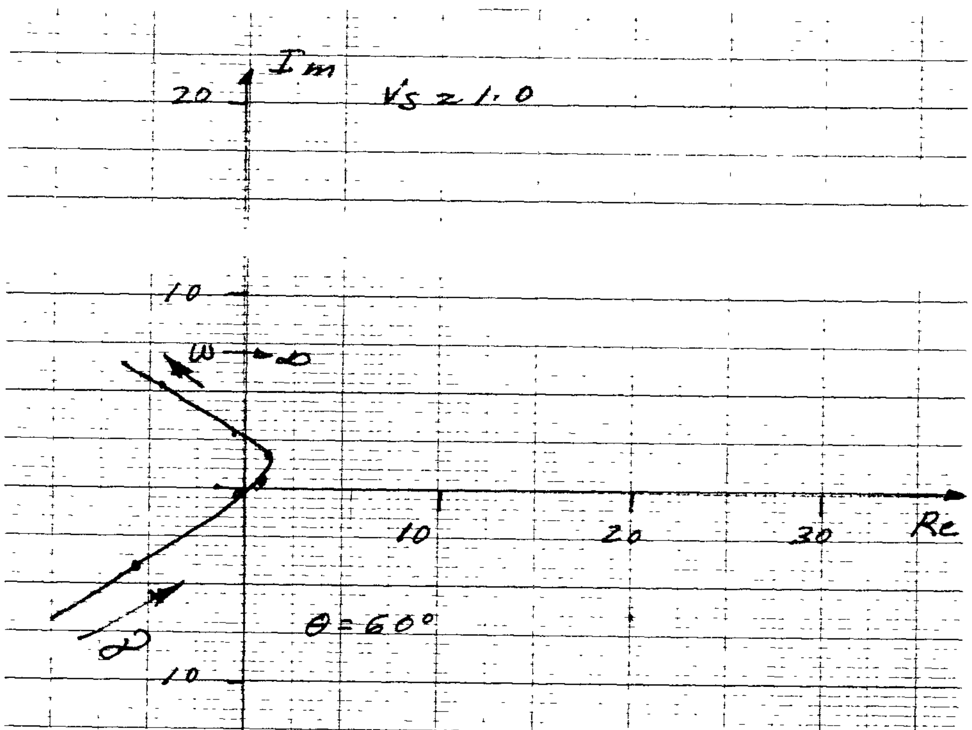

Figure 27.h

Once the stability limit for the uncompensated case was determined, series compensation was added to segments 2 and 3 one at a time. The previously defined procedure was again applied to each of the compensation cases, previously described, to determined the P_{SSL} and P_{max} values. Also as indicated before, different locations were tested on each line to determine the optimum location. Optimum location is defined to be the place where the highest P_{SSL} value was obtained for the same compensation.

5.2 Effect of Series Compensation on Power Stability Limits: Location and Degree of Compensation

The effect of location was evaluated by testing different locations for series compensation. The different locations were described already in chapter 4. Table 5.1 shows the results of the different locations tested.

TABLE 5.1

20% COMPENSATION of MSU-1 and MSC-7040 LINES

			Vs = 1.0 p.u.		Vs = 1.05 p.u.	
			P_{SSSL}	P_{max}	P_{SSSL}	P_{max}
Uncompensated Network			23.098	28.1907	24.545	29.60
COMPENSATION	MSU-1	Source	24.37	30.116	26.224	31.62
		Load	24.105	29.79	25.837	31.277
		Divided in half at both Ends	24.24	29.96	26.08	31.454
		Middle of the Line	24.35	30.12	26.202	31.621
	MSC-7040	Source	23.439	28.97	25.22	30.413
		Load	23.43	28.95	25.21	30.40
		Divided in half at both Ends	23.435	28.96	25.215	30.41
		Middle of the Line	23.44	28.968	25.223	30.41

From Table 5.1, it was determined that the optimum compensation location for the MSU-1 and MSC-7040 lines were at the source side. It was then decided that further compensation studies will be carried on the MSU-1 line, which lies in NYPA territory.

The results of the different degrees of compensation at the source side of the MSU-1 line, based on its own line impedance, are tabulated on Table 5.2. Figure 28, which was developed from Table 5.2, compares the P_{SSSL} for different degrees of compensation for V_S equal to 1.0 and 1.05 p.u.

TABLE 5.2

MSU-1 COMPENSATION AT SOURCE

	Vs = 1.0 p.u.		Vs = 1.05 p.u.	
Degree of Compensation	P_{SSSL}	P_{max}	P_{SSSL}	P_{max}
20%	24.35	30.1163	26.224	31.622
40%	25.489	32.337	27.821	33.95
60%	27.13	34.9	29.277	36.65
80%	29.047	37.9	31.37	39.8

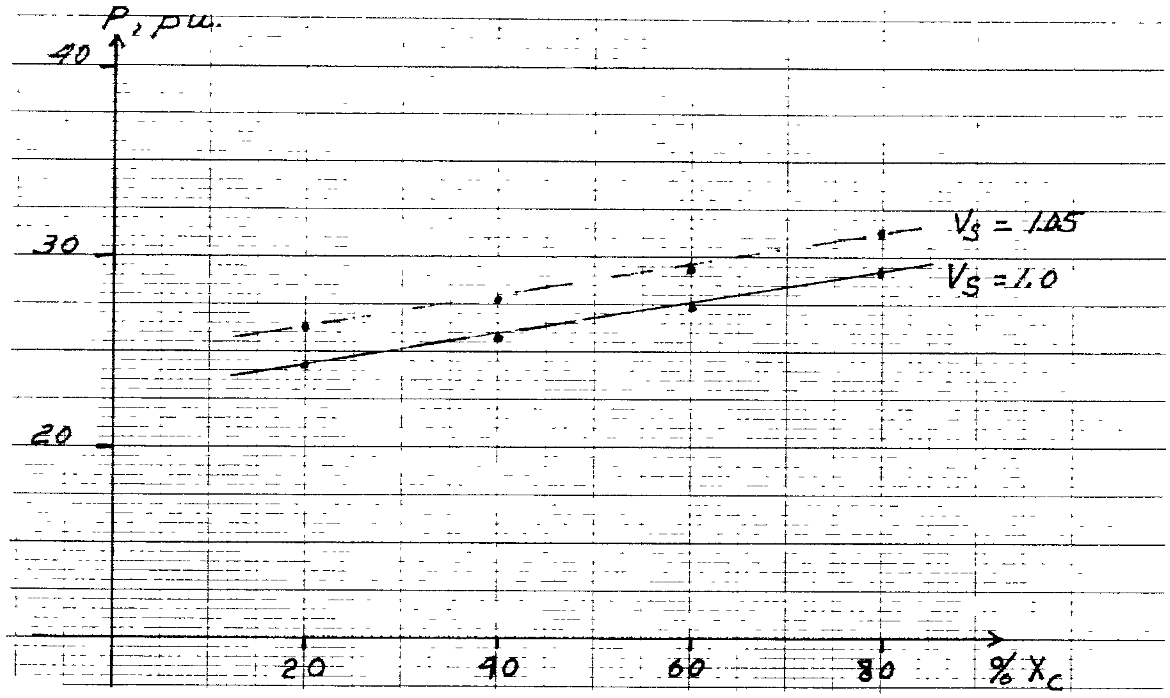

Figure 28

Another way to evaluate the P_{SSSL} improvement when compensating a power network is to compare power gain improvement against degree of compensation. The power gain is defined as the ratio of the compensated P_{SSSL} to the P_{SSSL} of the uncompensated case.

$$\text{Power Gain} = G_P = \frac{P_{SSSL(comp)}}{P_{SSSL(uncomp)}} \times 100\%$$

Figure 29 presents the power gain of self compensation of the MSU-1 line at its source side.

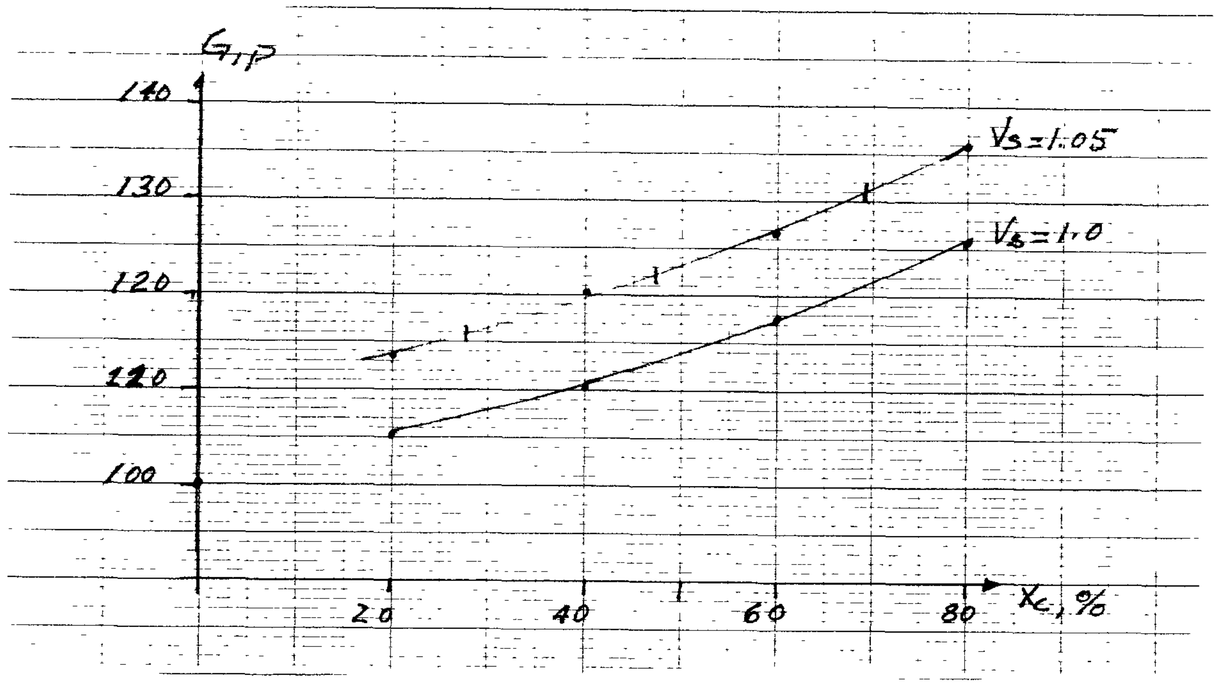

Figure 29

Next, 20%, 40%, 60% and 80% compensation of the total line impedance of segments 2 and 3 were placed on the source side of the MSU-1 line. Table 5.3 tabulates these results. As in the previous cases, figure 30 was developed to compare the different P_{SSSL} levels.

TABLE 5.3

OVERALL TRANSMISSION LINE COMPENSATION LOCATED AT THE SOURCE SIDE OF MSU-1

	Vs = 1.0 p.u.		Vs = 1.05 p.u.	
Degree of Compensation	P_{SSSL}	P_{max}	P_{SSSL}	P_{max}
20%	24.759	30.993	26.665	32.54
40%	27.126	34.414	29.24	36.13
60%	29.63	38.68	32.01	40.61
80%	32.3	44.15	35.523	46.36

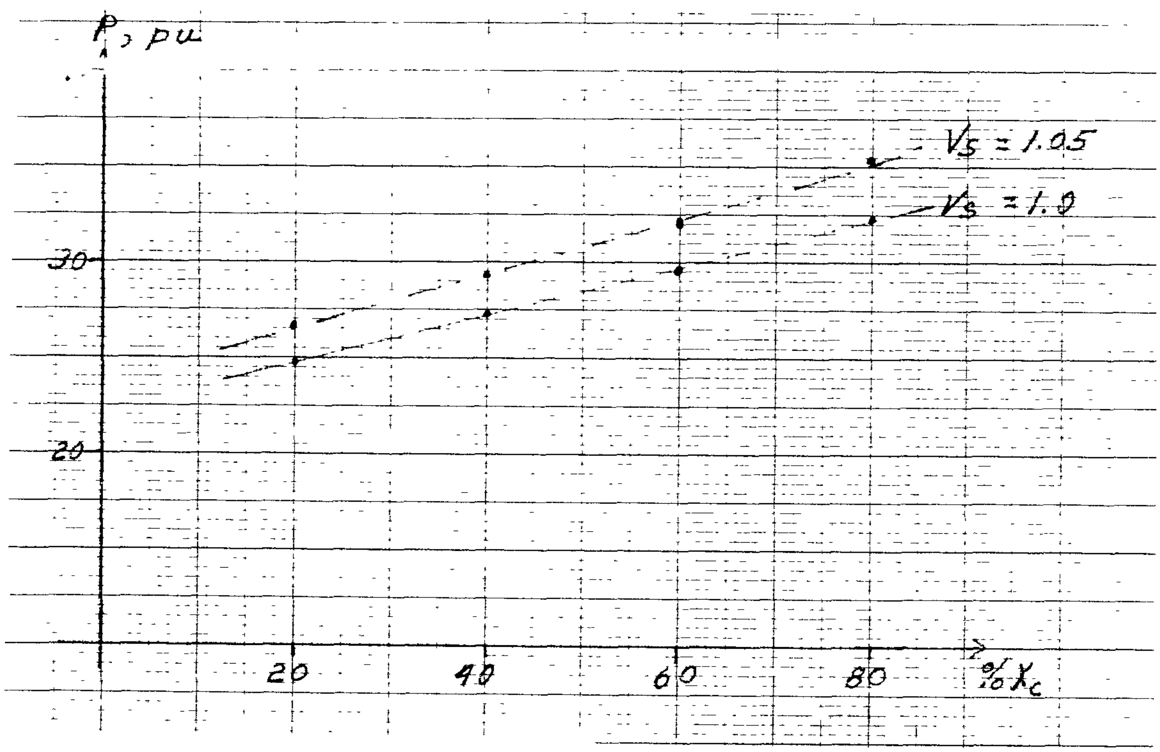

Figure 30

Similarly to the power gain comparisong of table 5.2 a power gain comparisong is presented for table 5.3 in Figure 31.

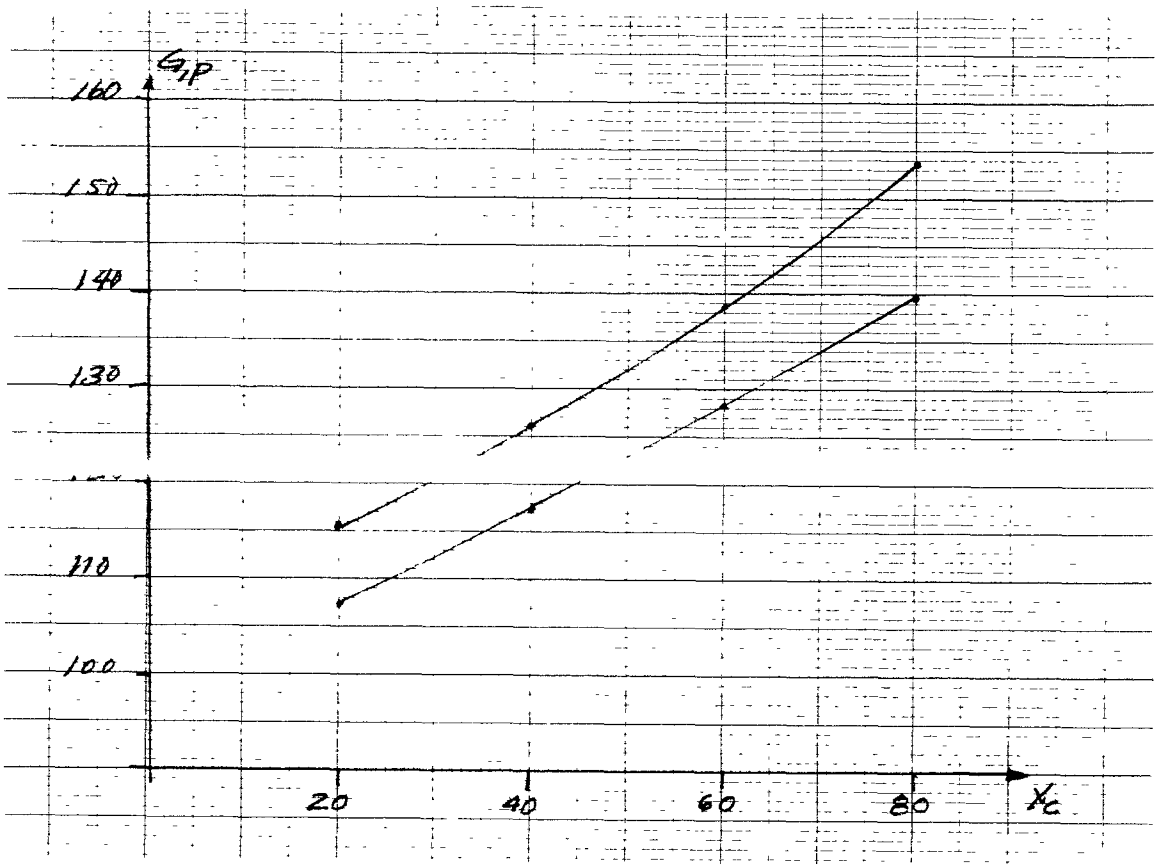

Figure 31

A final compensation test with the overall percent compensation was done by placing the series capacitance in the physical center of the MSU-1 and MSC-7040 lines. The physical center was found to be 39 miles south of the Massena substation. To study these cases, the modeling of the network was modified. The MSU-1 line was now modeled in two segments. The new segment 3 represented 29.16% of the MSU-1 line, segment 2 represented the remaining 70.84% of the line. The accuracy of the new model was validated by comparing the overall ABCD parameters for the four segments with no compensation against the original three segment uncompensated overall ABCD. The results of these cases are tabulated on Table 5.4.

TABLE 5.4

OVERALL TRANSMISSION LINE COMPENSATION
LOCATED AT PHYSICAL TRANSMISSION CENTER

	Vs = 1.0 p.u.		Vs = 1.05 p.u.	
Degree of Compensation	P_{SSSL}	P_{max}	P_{SSSL}	P_{max}
20%	27.01	34.26	29.113	35.975
40%	29.57	38.60	31.94	40.525
60%	32.86	44.158	35.53	46.37
80%	37.132	51.603	40.278	54.183

Figure 32 is the compensation characteristic of Table 5.4 for V_s equal to 1.0 and 1.05 p.u. Figure 33 is the power gain characteristic for this case.

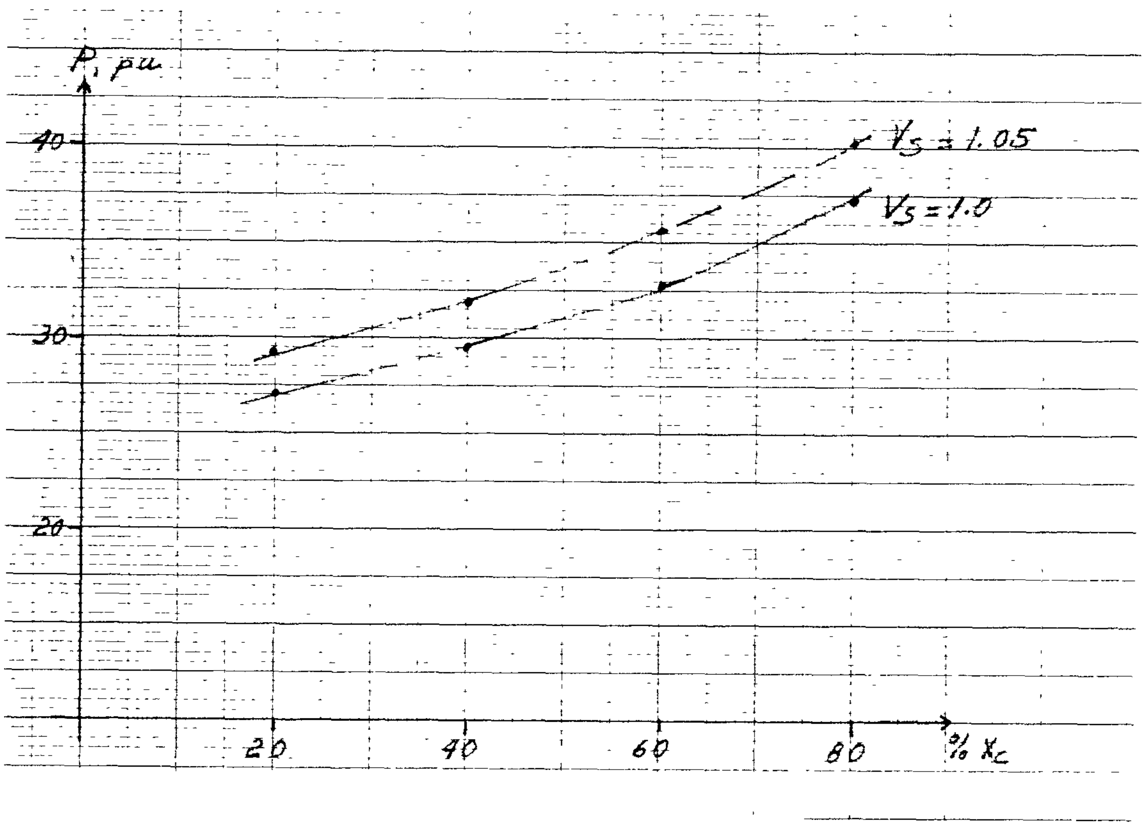

Figure 32

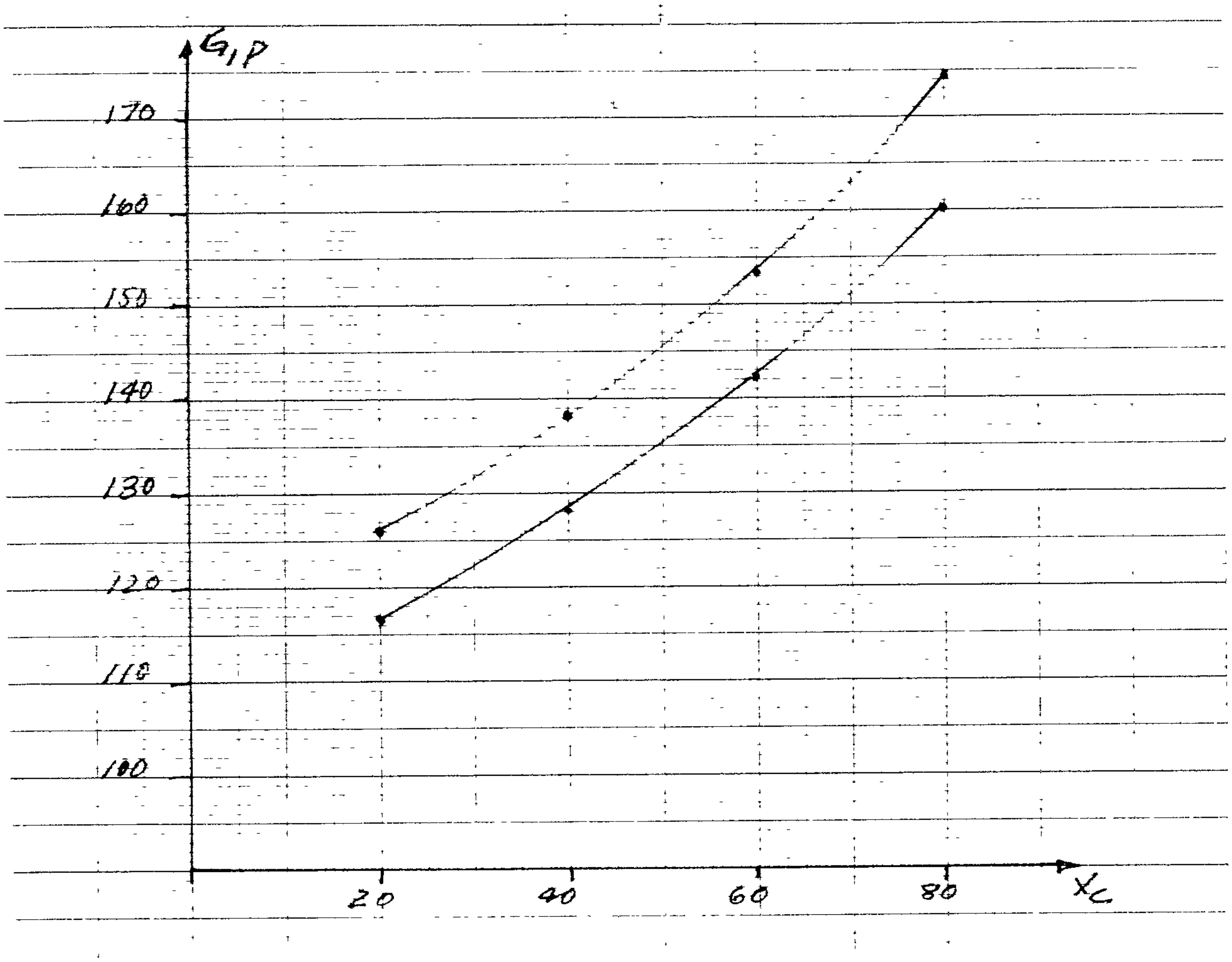

Figure 33

5.3 Effect of Compensation on the Network Natural Frequency

As it was defined in chapter 2, the natural frequency of the compensated line can be determined by equation 2.8, which is repeated below.

$$f_n = f\sqrt{\frac{X_c}{X_1}}$$

For the system studied x_1 is the overall impedance of the uncompensated case, whic is 0.017699 p.u.

The subsynchronous frequencies for the self-compensation case of the MSU-1 line at the source side. Are presented below on table 5.4.

Table 5.3

% X_c	f_n
14	22.55 hz
28	31.95 hz
43	39.14 hz
57	45.19 hz

The subsynchronous frequencies for the compensation of the 765 kV line with the overall values is presented in table 5.6.

Table 5.6

% X_c	f_n
20	26.8 hz
40	37.9 hz
60	46.5 hz
80	53.7 hz

Figure 34 compares the subsynchronous frequencies of tables 5.5 and 5.6.

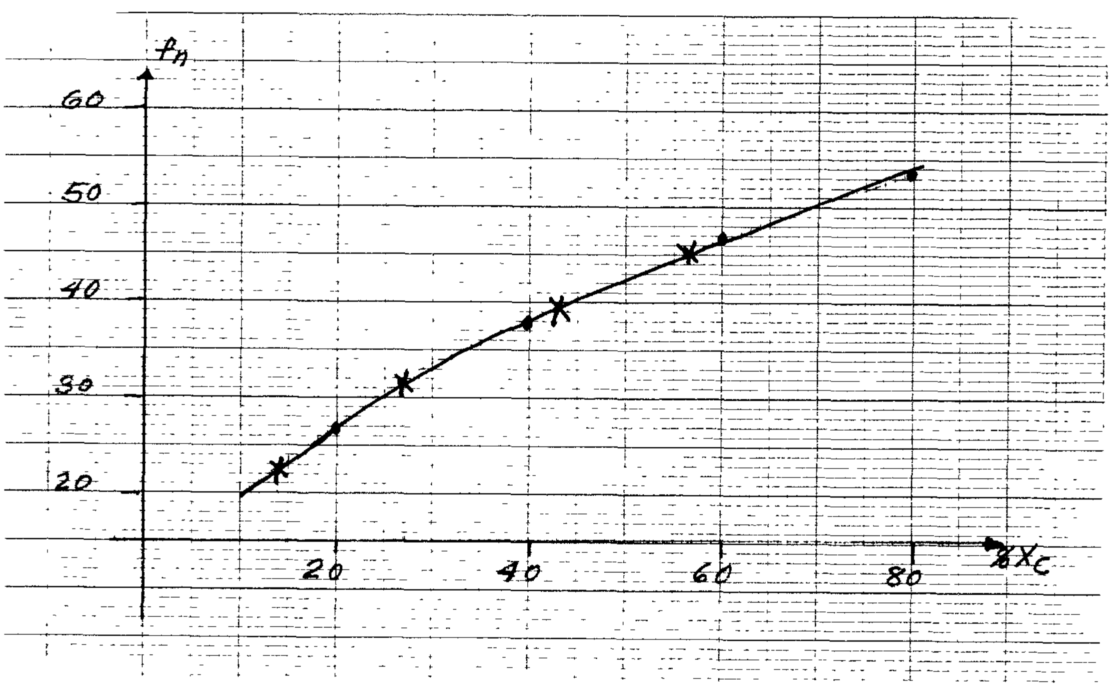

Figure 34

From figure 34 we can determine that by going to a higher degree of compensation the subsynchronous frequencies of the network are the same as when adding lower compensation on the MSU-1 line. Therefore attention to higher degrees of compensation is recommended.

CHAPTER VI

Conclusions

Hydro-Quebec's Beauharnois generating units together with the New York Power Authority 765 kV power transmission system was investigated for possible improvement in Power Steady State Stability Limits (P_{SSSL}) by adding series capacitive compensation. The actual stability limits were compared with the theoretical power limits. The frequency domain technique was used to obtain the stability characteristics at any operating condition. The following findings were obtained:

1. The actual P_{SSSL} of an existing uncompensated power system with an dwithout increasing the system operating voltage are presented in table 5.1.

2. Next, several locations of the 765 kV power network were studied to determine the optimun location of series capacitive compensation for the system under investigation.

Based on the results presented in table 5.1 it was found that series capacitance when installed at the so urce side of the MSU-1 line yielded a higher degree of power gain.

3. The effect of increasing the degree of compensation at the above indicated location of the MSU-1 line showed continued increase in the system's P_{SSSL} *value.*

4. Following Kimbark's recommendation [3] for line compensation location, series compensation was applied to the center of the H-Q NYPA 765 kV system. This new location for compensation yielded higher P_{SSSL} *values for the power system studied. This results are presented in table 5.4.*

5. Also it is seen that the system's natural Subsynchronous frequency increases in proportion to the amount of compensation as shown in figure 34.

6. The best location for series compensation for the power system investigated is recommended to be the physical center of the MSU-1 and MSC-7040 transmission lines.

BIBLIOGRAPHY

[1] *IEEE Committee Report, "Computer Representation of Excitation Systems", IEEE Trans. Power App. Syst., June 1968*

[2] *N. Fahlen, G. Janke, O. Nerf, "Series Capacitors in Power Systems", IEEE Trans. Power App. Syst., May/June 1975*

[3] *E. W. Kimbark, "How to Improve System Stability Without Risking Subsynchronous Resonance", IEEE Trans. Power App. Syst., September/October 1977*

[4] *General Electric, "Transmission, a Magazine for Electrical Utilities, Transmission Line Compensation", March 1973*

[5] *General Electric, "The Amplidyne Characteristics and Technical Data", GET - 1985D*

[6] *IEEE Committee Report, "Excitation System Dynamic Characteristics", IEEE Trans. Power App. Syst., Jan/Feb 1973*

[7] IEEE Committee Report, "Dynamic Models for Steam and Hydro Turbines in Power System Studies", IEEE Trans. Power App. Syst., Nov./Dec. 1973

[8] G.D. Brewes, R.A. Gibley, "The Use of Series Capacitors to Obtain Maximum EHV Transmission Capability", IEEE Trans. Power App. Syst., Nov.1964

[9] E.W. Kimbark, "Improvement of System Stability by Switched Service Capacitors", IEEE Trans. Power App. Syst., Feb. 1966

[10] L.A. Kilgne, L.C. Elliott, E.R. Taylor, "The Prediction and Control of Self Excited Oscillators Due to Series Capacitors in Power Systems", IEEE Trans. Power App. Syst., May/June 1971

[11] N. deFranco, A. Clerici, P. Thanassoulis, "Overvoltages on a Series Compensated 750Kv System for the 10,000MW Itaipu Project", IEEE Trans. Power App. Syst., March/April 1975

[12] *G. Alexander, J.G. Andrichak, S.D. Rowe, S.B. Wilkingson, "Series Compensated Line Protection: A Practical Evaluation", Presented to the Pennsylvania Electric Association, 1989*

[13] *IEEE Committee Report, "Proposed Terms and Definitions for Subsynchronous Oscillations", IEEE Trans. Power App. Syst., March/April 1980*

[14] *V.A. Venikov, "Transient Process in Electrical Power Systems", Mir Publishers, Moscow, 1980*

[15] *P.M. Andersen, A.A. Fouad, "Power System Control and Stability", vol. 1, Iowa State University Press, Ames, Iowa, 1977*

[16] *M.V. Meerov, "Introduction to the Dynamics of Automatic Regulating in Electrical Machines", Butterworth, London, England, 1961*

[17] *E.W. Kimbark, "Power System Stability", vol. I, Elements of Stability Calculations, John Wiley & Sons, Inc., New York, 1948*

[18] C.A. Gross, "Power System Analysis", 2nd edition, John Wiley & Sons, Inc., New York, 1986

[19] W.D. Stevenson, "Elements of Power System Analysis", 3rd edition, McGraw-Hill, New York, 1975

[20] G.M. Swisher, "Introduction to Linear System Analysis", Matrix Publisher, Inc., Cleveland, Ohio, 1976

[21] S. B. Pandey, "Class Notes EE711: Stability and Dynamics of Power Networks", New Jersey Institute of Technology, Newark, NJ, Spring, 1990

[22] S.M. Pandey, H.J. Candia,"Scope of the Frequency Domain Technique in Evaluation of Power System Stability", Presented at the Twenty Second Modelling and Simulation Coference at the School of Engineering of the University of Pittsburgh, May 1991.

APPENDIX I

Beauharnois Generator Data

		TURBINE						ALTERNATEUR						
NO.	MISE EN SERVICE	MARQUE	TYPE	HAUTEUR DE CHUTE M	VITESSE REV/M	PUISSANCE HP	MW	MARQUE	TENSION VOLTS	COURANT AMP.	PUISSANCE APPARENTE KVA	FACTEUR DE PUISSANCE	Mvar	PUISSANCE ACTIVE KW
1	SEPT.'32 ✓	DEW	F	24.39	75	64,800	48,3	GE	13,800	2,300	55,0	.80	33	44,0
2	SEPT.'32 ✓	DEW	F	24.39	75	53,000	39,5	GE	13,200	2,025	46,625	.80	28	37.300
3	MAI'82 ✓	DEW	F	24.39	75	64,800	48,3	GE	13,800	2,300	55,0	.80	33	44,0
4	SEPT.'81 ✓	DEW	F	24.39	75	64,800	48,3	GE	13,200	2,025	46,625	.80	28	37,300
5	JANV.'39 ✓	DEW	F	24.39	75	53,000	39,5	GE	13,200	2,025	46,625	.80	28	37,300
6	AOUT'41 ✓	DEW	F	24.39	75	53,000	39,5	GE	13,200	2,025	46,625	.80	28	37,300
7	NOV.'41 ✓	DEW	F	24.39	75	53,000	39,5	GE	13,200	2,025	46,625	.80	28	37,300
8	NOV.'48 ✓	DEW	F	24.39	75	53,000	39,5	GE	13,200	2,025	46,625	.80	28	37,300
9	OCT.'32 ✓	DEW	F	24.39	75	53,000	39,5	GE	13,800	2,090	50,000	.80	30	40,000
10	SEPT.'32 ✓	DEW	F	24.39	75	53,000	39,5	GE	13,800	2,090	50,000	.80	30	40,000
11	OCT.'34 ✓	DEW	F	24.39	75	53,000	39,5	O	13,800	2,090	50,000	.80	30	40,000
12	AVRIL'35 ✓	DEW	F	24.39	75	53,000	39,5	GE	13,800	2,090	50,000	.80	30	40,000
13	DEC.'35 ✓	DEW	F	24.39	75	53,000	39,5	GE	13,800	2,090	50,000	.80	30	40,000
14	SEPT.'83 ✓	DEW	F	24.39	75	64,800	48,3	GE	13,800	2,090	50,000	.80	30	40,000
15	DEC.'50 ✓	DEW	F	23.78	75	55,000	41,0	W	13,800	2,090	50,000	.80	30	40,000
16	DEC.'50	AC	F	23.17	75	56,000	41,8	GE	13,800	2,155	51,400	.80	31	41,120
17	AVRIL'51 ✓	DEW	F	23.78	75	55,000	41,0	W	13,800	2,090	50,000	.80	30	40,000
18	OCT.'51	AC	F	23.17	75	56,000	41,8	GE	13,800	2,155	51,400	.80	31	41,120
19	AVRIL'83 ✓	DEW	F	23.78	75	64,800	48,3	W	13,800	2,090	50,000	.80	30	40,000
20	DEC.'51	AC	F	23.17	75	56,000	41,8	GE	13,800	2,155	51,400	.80	31	41,120
21	NOV.'53 ✓	DEW	F	23.78	75	55,000	41,0	GE	13,800	2,090	50,000	.80	30	40,000
EAST 22	AOUT'53	AC	F	23.17	75	56,000	41,8	GE	13,800	2,090	50,000	.80	[illegible]	40,000
WEST 23	AOUT.'83 ✓	DEW	F	23.78	75	64,800	48,3	W	13,800	2,445	57,060	.80	34	46,750
24	JANV.'53	AC	F	23.17	75	56,000	41,8	W	13,800	2,090	50,000	.80	30	40,000
25	AOUT'52 ✓	DEW	F	23.78	75	55,000	41,0	GE	13,800	2,090	50,000	.80	[illegible]	40,000
26	OCT.'52	AC	F	23.17	75	56,000	41,8	GE	13,800	2,090	50,000	.80	32	40,000
27	SEPT.'59	EE	H	23.78	94.7	73,700	55,0	W	13,800	2,720	65,000	.85	34	55,250
28	JUILL.'59	EE	H	23.78	94.7	73,700	55,0	W	13,800	2,720	65,000	.85	34	55,250
29	SEPT.'59	EE	H	23.78	94.7	73,700	55,0	W	13,800	2,720	65,000	.85	34	55,250
30	NOV.'59	EE	H	23.78	94.7	73,700	55,0	W	13,800	2,720	65,000	.85	34	55,250
31	DEC.'59	EE	H	23.78	94.7	73,700	55,0	W	13,800	2,720	65,000	.85	34	55,250
32	MAI'60	EE	H	23.78	94.7	73,700	55,0	W	13,800	2,720	65,000	.85	34	55,250
33	JUILL.'60	EE	H	23.78	94.7	73,700	55,0	W	13,800	2,720	65,000	.85	34	55,250
34	OCT.'60	EE	H	23.78	94.7	73,700	55,0	W	13,800	2,720	65,000	.85	[illegible]	55,250
35	JANV.'61	EE	H	23.78	94.7	73,700	55,0	W	13,800	2,720	65,000	.85	[illegible]	55,250
36	AVRIL'61	EE	H	23.78	94.7	73,700	55,0	W	13,800	2,720	65,000	.85	[illegible]	55,250
TOTAL														

LES CARACTERISTIQUES ORIGINALES DES GROUPES SONT DONNEES A LA PAGE SUIVANTE.

○ Limitation de transformateur

T1 et T3 = 46.6 MVA

T23 = 50 MVA

$X_d = .39$

$X_d'' = .27$

APPENDIX II

Beauharnois Step-Up Transformer Data

BEAUHARNOIS
TRANSFORMER BANKS (1)

No.	R	Z	Im (2)	Nomind Rating		Off load Tap			
	%	%	%	kV_H/kV_L	MVA 3φ	Position			
	Based on Nominal kV and MVA					1	2	3	4
T1	0,571	8,41	1,1112	127,41/13,2	46,5	133,84	127,41	120,98	
T2	0,418	10,[illegible]	2,5600	"	65,0	"	"	"	114,55
T3	0,660	8.35	0,8408	"	46,5	"	"	"	
T4	0,664	8 40	0,8408	"	"	"	"	"	
T5	0,664	8.40	0,8408	"	"	"	"	"	114,55
T6	0,664	8,40	0,8408	"	"	"	"	"	"
T1E	0,674	8.43	0,8408	"	"	"	"	"	"
T7 (3)	0,300	12,00 (4)	0,7500	127,4/13,2	100,0	133,77	127,4	121,03	114,97
T10 (3)	0,300	12,00 (4)	0,7500	"	"	"	"	"	"
T11	0,700	10.05	0,7166	127,41/13,2	50,0	133,84	127,41	120,98	114,55
T12	0,700	10.05	0,7166	"	"	"	"	"	"
T13	0,682	9,88	0,7166	"	"	"	"	"	"
T14	0,706	10.00	0,7166	"	"	"	"	"	"
T15	0,684	9,23	0,7444	"	"	"	"	"	"
T16	0,698	9,23	0,6905	"	"	"	"	"	"
T17	0,698	9,17	0,7339	"	"	"	"	"	"
T18	0,702	9,18	0,7280	"	"	"	"	"	"
T19	0,720	9,28	0,6484	"	"	"	"	"	"
T20	0,732	9,28	0,7545	"	"	"	"	"	"
T21	0,716	9,41	0,6873	"	"	"	"	"	"
T22	0,728	9,55	0,5700	"	"	"	"	"	"
T23	0,704	9,37	0,5853	"	"	"	"	"	"
T24	0,726	9,30	0,6383	"	"	"	"	"	"
T25	0,704	9,36	0,5944	"	"	"	"	"	"
T26	0,704	9,94	0,5970	"	"	"	"	"	"
T27	0,420	10,11	2,230	"	65,0	"	"	"	"
T28	0,408	10,04	3,040	"	"	"	"	"	"
T29	0,434	10,09	2,390	"	"	"	"	"	"
T30	0,415	10,03	2,470	"	"	"	"	.	..
T31	0,432	10,00	2,190	"	"	"	"	"	"
T32	0,342	10,06	1,150	"	"	"	"	"	"
T33	0,340	10,02	0,965	"	"	"	"	"	"
T34	0,343	10,00	1,100	"	"	"	"	"	"
T35	0,348	10,00	1,100	"	"	"	"	"	"
T36	0,346	10,10	1,000	"	"	"	"	"	"

NOTES:

(1) Reference: Banque de données des rapports d'essai des transformateurs, service Etudes de réseaux, direction Planification, 82-04-22

(2) Magnetization current in % at nominal voltage ratio.

(3) New double secondary windings transformer (see operating single line diagram, enclosure 1-1)

(4) Value corresponding with the two secondary windings in service (parallel); with one secondary winding out of service, Z = 16% on 127,4/13,2 kV and 100 MVA bases.

(5) XXXX: estimated or typical values.

André Venne, ing.

AV/ja
revised 82-05-20

APPENDIX III

MSU-1 and MSC-7040 Transmission Line Parameters

MASSENA-MARCY 765 kV LINE

ELECTRICAL CHARACTERISTIC (134 miles)

Item No.	Item	Data
1.	Operating Voltage	
1a.	Nominal operating voltage	765 kV
1b.	Maximum operating voltage	800 kV
2.	Insulation level	
2a.	Impulse insulation level	2800 kV Pos.
2b.	Switching surge insulation level	1640 kV
2c.	60 Hertz insulation level	1730 kV Dry
3.	Circuit resistance, percent on 100 MVA base at nominal voltage, @ 50°C	
3a.	R1=	0.0479
3b.	R0=	1.133
4.	Circuit reactace, percent on 100 MVA base at nominal voltage	
4a.	X1=	1.255
4b.	X0=	3.600
5.	Circuit shunt capacitance, percent on 100 MVA base at nominal voltage	
5a.	Xc1=	16.23
5b.	Xc0=	23.98
6.	Circuit three phase line charging MVAR at nominal voltage, (without reactors in service)	616
7.	System 1 line protective relaying	Solid State directional comparison pilot system utilizing power line carrier.

MASSENA - CHATEAUGUAY 765 KV LINE
SUMMARY SHEET (ALSO SEE INDIVIDUAL LINE SECTIONS)

ELECTRICAL CHARACTERISTIC (55 miles)

Item No.	Item	Data
1.	Operating Voltage	
1a.	Nominal operating voltage	765 kV
1b.	Maximum operating voltage	800 kV
2.	Insulation level	
2a.	Impulse insulation level	2800 kV Pos.
2b.	Switching surge insulation level	1640 kV
2c.	60 Hertz insulation level	1730 kV Dry
3.	Total circuit resistance, percent on 100 MVA base at nominal voltage, @ 50°C	
3a.	R1=	0.02161
3b.	R0=	0.4651
4.	Total circuit reactance, percent on 100 MVA base at nominal voltage	
4a.	X1=	0.5149
4b.	X0=	1.477
5.	Total circuit shunt capacitance, percent on 100 MVA base at nominal voltage	
5a.	Xc1=	39.54
5b.	Xc0=	58.43
6.	Total circuit three phase line charging MVAR at nominal voltage (without reactors in service)	254
7.	System 1 line protective relaying	Solid state directional comparison pilot system utilizing powerline carrier
8.	System 2 line protective relaying	Solid state directional distance mho type
9.	Communication channels	Powerline carrier-two independent dual channel systems

APPENDIX IV

Parameters of System Study (all in p.u.)

Hydrogenerator Equivalent

M	0.00522
T_{do}	5.9761
X_d	0.0566
X_{eq}	0.03626
X'_d	0.039

Excitation Control System Equivalent

K_e	1.0
T_{do}	5.9761
T_e	1.4
T_3	0.4

MSU-1 Line

R	0.000479
X	0.01255
B	6.1614

MSC-7040 Line

R	0.0002161
X	0.005149
B	0.000253

H-Q Equivalent Network

R	*0.0011826*
X	*0.019522*
B	*0.0*